Bioorganic & Medicinal Chemistry 23 (2015) 5891–5908

Contents lists available at ScienceDirect

Bioorganic & Medicinal Chemistry

journal homepage: www.elsevier.com/locate/bmc

Exploration of the nicotinamide-binding site of the tankyrases, identifying 3-arylisoquinolin-1-ones as potent and selective inhibitors in vitro

Helen A. Paine [a], Amit Nathubhai [a], Esther C. Y. Woon [a,b], Peter T. Sunderland [a], Pauline J. Wood [a], Mary F. Mahon [c], Matthew D. Lloyd [a], Andrew S. Thompson [a], Teemu Haikarainen [d], Mohit Narwal [d], Lari Lehtiö [d], Michael D. Threadgill [a,*]

[a] Medicinal Chemistry, Department of Pharmacy & Pharmacology, University of Bath, Claverton Down, Bath BA2 7AY, UK
[b] Department of Pharmacy, National University of Singapore, Block S4, Science Drive 4, Singapore 117543, Republic of Singapore
[c] X-ray Crystallographic Suite, Department of Chemistry, University of Bath, Claverton Down, Bath BA2 7AY, UK
[d] Biocenter Oulu and Faculty of Biochemistry and Molecular Medicine, University of Oulu, Oulu, Finland

ARTICLE INFO

Article history:
Received 27 April 2015
Revised 24 June 2015
Accepted 25 June 2015
Available online 2 July 2015

Keywords:
Tankyrase
TNKS
Naphthyridinone
7-Aryl-1-methyl-1,2,3,4-tetrahydro-1,6-naphthyridin-5-one
Crystal structure

ABSTRACT

Tankyrases-1 and -2 (TNKS-1 and TNKS-2) have three cellular roles which make them important targets in cancer. Using NAD^+ as a substrate, they poly(ADP-ribosyl)ate TRF1 (regulating lengths of telomeres), NuMA (facilitating mitosis) and axin (in *wnt*/β-catenin signalling). Using molecular modelling and the structure of the weak inhibitor 5-aminoiso quinolin-1-one, 3-aryl-5-substituted-isoquinolin-1-ones were designed as inhibitors to explore the structure–activity relationships (SARs) for binding and to define the shape of a hydrophobic cavity in the active site. 5-Amino-3-arylisoquinolinones were synthesised by Suzuki–Miyaura coupling of arylboronic acids to 3-bromo-1-methoxy-5-nitro-isoquinoline, reduction and O-demethylation. 3-Aryl-5-methylisoquinolin-1-ones, 3-aryl-5-fluoroisoquinolin-1-ones and 3-aryl-5-methoxyisoquinolin-1-ones were accessed by deprotonation of 3-substituted-*N*,*N*,2-trimethylbenzamides and quench with an appropriate benzonitrile. SAR around the isoquinolinone core showed that aryl was required at the 3-position, optimally with a *para*-substituent. Small *meta*-substituents were tolerated but groups in the *ortho*-positions reduced or abolished activity. This was not due to lack of coplanarity of the rings, as shown by the potency of 4,5-dimethyl-3-phenylisoquinolin-1-one. Methyl and methoxy were optimal at the 5-position. SAR was rationalised by modelling and by crystal structures of examples with TNKS-2. The 3-aryl unit was located in a large hydrophobic cavity and the *para*-substituents projected into a tunnel leading to the exterior. Potency against TNKS-1 paralleled potency against TNKS-2. Most inhibitors were highly selective for TNKSs over PARP-1 and PARP-2. A range of highly potent and selective inhibitors is now available for cellular studies.

1. Introduction

Tankyrase-1 (PARP-5a, TNKS-1, ARTD5) and tankyrase-2 (PARP-5b, TNKS-2, ARTD6) are members of the poly(ADP-ribose)polymerase (PARP) superfamily of enzymes, which attract considerable current interest owing to their roles at telomeres and involvement at the mitotic spindle and in the *wnt* signalling pathway. TNKS-1 was first reported in 1998,[1] as regulating the lengths of telomeres through poly(ADP-ribosyl)ation of telomere repeat binding factor-1 (TRF-1) and autopoly(ADP-ribosyl)ation.[2,3] NAD^+ is the source of the ADP-ribose (ADPr) units, as for other PARPs.[4] TNKS-1 is also responsible for poly(ADP-ribosyl)ating NuMA at the mitotic spindle, ensuring its correct functioning during mitosis.[5] Furthermore, TNKS-1 is a component of the *wnt* signalling system, where it poly(ADP-ribosyl)ates axin. Poly(ADPr)-axin is thus tagged for ubiquitinylation and destruction through the proteasome, increasing the levels of β-catenin, while decreasing the levels of phosphorylated β-catenin.[6,7] Accumulation of β-catenin leads to a proliferative signal in the nucleus.[7] The closely structurally related isoform TNKS-2 can substitute for TNKS-1 in many, but not all, of these activities.[2,8,9]

Telomeres are protected by the shelterin complex of six telomere-specific proteins. Its main role is to protect the telomere from being recognised as a site of damage by the DNA-repair machinery,

* Corresponding author. Tel.: +44 1225 386840; fax: +44 1225 386114.
E-mail address: m.d.threadgill@bath.ac.uk (M.D. Threadgill).

http://dx.doi.org/10.1016/j.bmc.2015.06.061
0968-0896/

thus preventing inappropriate recombination events.[10] Two shelterin proteins, TRF-1 and TRF-2, localise to the telomeres, maintaining t/d-loop structures and binding directly to double-stranded TTAGGG repeats.[11] DNA polymerases cannot replicate fully to the ends of linear DNA, so the telomere acts as a sacrificial entity; a critical length is eventually reached, eliciting a DNA-damage checkpoint response, through p53, and subsequent replicative senescence or apoptosis.[12,13] Proliferating cells use telomerase to re-lengthen the telomeric DNA. TRF-1 binds to the telomere preventing access by telomerase. Poly(ADP-ribosyl)ation of TRF-1 by TNKS-1 causes it to dissociate from telomeric DNA, leading to ubiquitinylation and destruction of the TRF-1 and allowing telomerase access to the DNA.[1] TNKS-1 may also have a role in response to DNA damage at telomeres.[14] During mitosis, TNKS-1 is present at the ends of interphase chromosomes,[5,15] bound to nuclear mitotic apparatus protein (NuMA), which accumulates around the pericentriolar matrix.[16] Under the possible regulation of GSK3,[17] TNKS-1 poly(ADP-ribosyl)ates NuMA. siRNA knock-down of TNKS-1 causes mitotic arrest in HeLa cells.[18] Similar removal using RNAi caused post-anaphase arrest.[19] A critical role of TNKSs in mitosis is in resolution of the telomeres.[13,18,19]

TNKSs are over-expressed in several clinical cancers and cancer cell lines, including breast cancer,[20,21] colon cancer,[22,23] chronic myeloid leukaemia,[24] brain tumours,[25,26] and gastric[27] and bladder cancers,[28] pointing to one or more critical roles. Seimiya[29] proposed them as therapeutic targets on the basis of their roles at telomeres. Subsequent revelation of the roles of TNKSs in *wnt* signalling[7] and the observation of aberrant *wnt* signalling in many tumour types[30] has reinforced their value as targets for anti-cancer drug design.[31,32] One TNKS inhibitor has shown activity in an APC-mutant mouse model of colon cancer.[33] The role of TNKS-1 in the replication of *Herpes simplex* virus may also point to applications in the treatment of viral infections.[34] These observations and opportunities point to the need for potent and selective inhibitors of the TNKSs and for a greater understanding of the detail of the binding pockets around the NAD$^+$-binding site.

Figure 1 shows the structures of some known inhibitors of the TNKSs. XAV939 **1**[7] and GM244-LM **2**[35] both bind at the nicotinamide-binding site, as do our 2-arylquinazolin-4-ones **3**[36,37] and flavones, including **4**.[38,39] Our lead water-soluble inhibitor of PARP-1 and PARP-2, 5-AIQ **11a**,[40–44] binds only weakly to the TNKSs, with IC_{50} in the low μM range (preliminary data not shown). Compound **5** binds with its quinazolin-4-one at the nicotinamide-binding site and the side-chain extending to make interactions in the adenosine-binding site of the NAD$^+$-binding cleft.[45] EB-47 **6** occupies both the nicotinamide- and adenosine-binding pockets but with a linker that uses a different path on the enzyme surface.[46] Compound **7** uses an amino-1,2,4-triazole to make the requisite H-bonds within the nicotinamide-binding site,[47] whereas **8** uses a dihydropyranopyrimidine to bind there.[48] IWR1 **9**[49] and G007-LK **10**[35,50] bind to the adenine-binding site alone.

We present here our structure-based design of 3-arylisoquinolin-1-ones as inhibitors of the TNKSs and our exploration of the structure–activity relationships (SARs) around this core and binding, guided by crystallography and studies in silico. Using rational modification of the substituents around the core, the aim of this study is to explore the detail of the conformational and space-filling requirements for optimum occupation of a large hydrophobic cavity in the enzymes adjacent to the nicotinamide-binding site.

2. Results and discussion

2.1. Design of inhibitors

The design of the isoquinolin-1-one inhibitors was approached from three start-points. Firstly, we solved the crystal structures of our water-soluble PARP-1 inhibitors **11a**,[40] **11b**,[51] **11c**,[51] and **11d**[52] (Fig. 1) bound into the NAD$^+$-binding site of the catalytic domain of human TNKS-2. These compounds were shown, in preliminary studies, to be weak inhibitors of the TNKSs (IC_{50} >10 μM) (data not shown). Secondly, the structure of XAV939 **1** bound into the catalytic domain of TNKS-2 is available.[53] Thirdly, we sought to investigate 'scaffold-hopping' from our 2-arylquinazolin-4-one inhibitors, from our preliminary studies,[36] to the 3-arylisoquinolin-1-ones.

Figure 2 shows images of the crystal structures of **11a–d** bound into the catalytic domain of human TNKS-2. Each shows binding

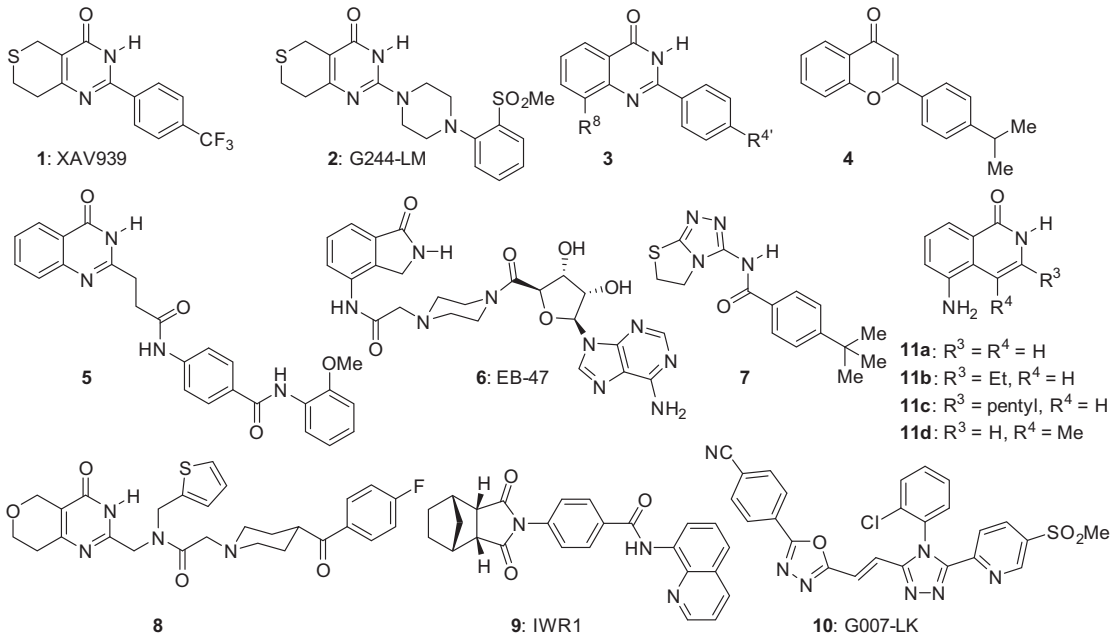

Figure 1. Structures of recently disclosed inhibitors of the TNKSs **1**–**10**, of our lead inhibitor of PARP-1 **11a** and of 5-amino-3/4-alkylisoquinolin-1-ones **11b–d** used in the initial crystallographic study.

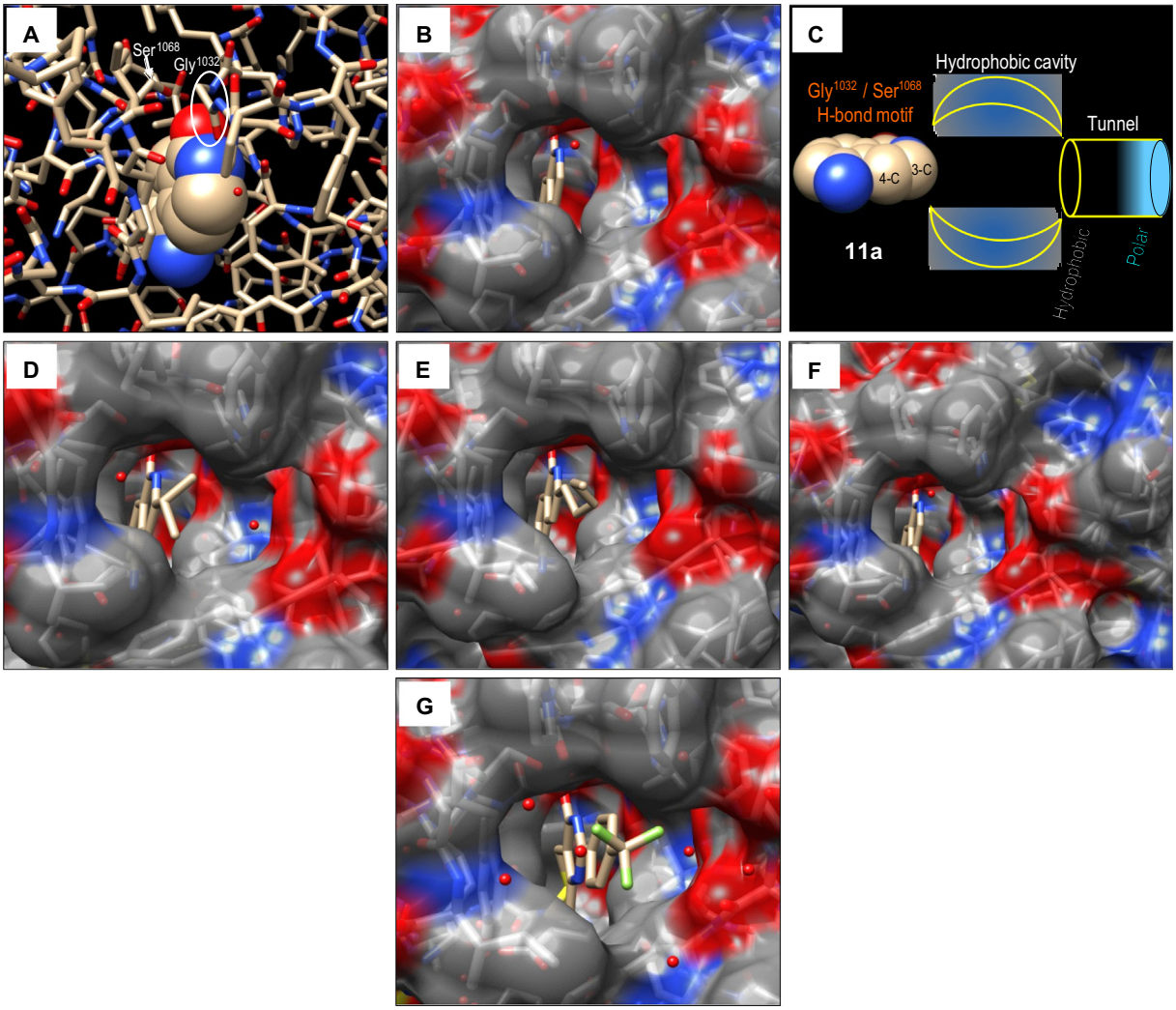

Figure 2. Crystal structures of (A) **11a**; (B) **11a**; (D) **11b**; (E) **11c**; (F) **11d** bound into the NAD^+-binding site of the catalytic domain of human TNKS-2. Panels A and B show the same view with different rendering, with A showing the classical PARP H-bonding motif and B emphasising the hydrophobic cavity and tunnel. Panel C shows a cartoon representation of the binding of **11a** and of the adjacent hydrophobic cavity and tunnel. Panel D shows the ethyl group of **11b** in two partly occupied conformations within the hydrophobic cavity. Panel G shows the corresponding structure of XAV939 **1** bound into tankyrase-2.[43]

into the NAD^+-binding site, mimicking nicotinamide. The principal binding contacts are H-bonds from N–H of the isoquinolin-1-one to the C═O of Gly^{1032} and from the O–H of Ser^{1068} and the N–H of Gly^{1032} to the C═O of the isoquinolinone. π-Stacking with the aromatic side-chain of Tyr^{1071} is also seen. This is the classical binding motif for most inhibitors of the PARP isoforms.[54,55] The 5-NH_2 of **11a**–**d** was accommodated in a small pocket and there was a small niche to accept the 4-methyl in **11d**. There is a large cavity adjacent to the 3-position of the isoquinolin-1-ones; the small 3-alkyl groups of **11b**,**c** were located in this cavity near to the entrance. The cavity is lined with aromatic and hydrophobic residues (mainly Pro^{1034}, Phe^{1035}, Tyr^{1050}, Tyr^{1071}), with a small tunnel leading from the far end of the hydrophobic cavity towards the exterior. The size and shape of the hydrophobic cavity suggest that it could accommodate a benzene ring, with modest substituents. A water molecule was evident in the centre in complexes of the 3-H isoquinolinones **11a**,**d**, whereas two water molecules were seen towards the sides of the cavity when it was partly occupied by ethyl in **11b**. The pentyl group in **11c** was too large to allow an ordered water molecule in the cavity. Figure 2C shows a cartoon of the arrangement of the hydrophobic cavity and the tunnel, relative to the H-bonding motif anchoring the lactam of **11a**.

The published crystal structure of **1** bound into the catalytic domain of TNKS-2 also shows the classical PARP-binding motif of three H-bonds from the ligand to Gly^{1032} and Ser^{1068}.[53] The 4-trifluoromethylphenyl group projects into the hydrophobic cavity, forming a π-stack with Tyr^{1050} and hydrophobic interactions with Pro^{1034}, Phe^{1035} and Ile^{1075}.[34] This fits well with our predictions from our results on the binding of **11a**–**d** with TNKS-2, in that the phenyl ring of **1** occupies much of the hydrophobic cavity and the trifluoromethyl group is located at the entrance to the tunnel.

The SAR from our preliminary study[36] on the 2-arylquinazolin-4-ones suggested that the lactam H-bonding motif was essential and that a *para*-substituted benzene ring could be accepted by the hydrophobic cavity. One example, (**3**: $R^{4'} = CH_2NHCbz$, $R^8 = Me$) projected deep into the tunnel, with only slight loss of activity. The preliminary SAR also suggested the need for a small substituent at the 8-position (R^8 in **3**, Fig. 1, corresponding to the 5-position in isoquinolin-1-ones (R^5 in **11**)). This SAR was rationalised by modelling studies.

The structures of the designed isoquinolin-1-ones **12**–**17** are shown in Figure 3. All contain the 3-arylisoquinolin-1-one core, as predicted by the structural studies and comparison with the

2-arylquinazolin-4-ones to be required. All carry a 5-substituent, as this was better in the quinazolin-4-ones.[36] However, the nature of the 5-substituent was not clearly predicted and comparison of compounds in the series **12**–**16** may clarify this. Compounds **12** and **16** have H-bond-donor electron-donating groups (EDGs) (the 5-NH_2 in **12** is unprotonated at physiological pH), whereas **15** contain a H-bond-acceptor EDG. Analogues **13** and **14** have non-polar 5-substituents, which is electron-neutral in **13** and electron-withdrawing in **14**. Within each series, especially **12** and **13**, the nature, size and location of the substituent on the 3-aryl group is explored. Substituents range from polar H-bond-donors (in **12p**,**t**,**u**), through H-bond-acceptors (in **12d**–**f**, **13d**, **14c**, **15h**) to non-polar groups and atoms (in **12b**,**c**,**g**–**n**, **13b**,**c**,**e**–**j**, **14b**,**d**–**g**, **15b**–**f**, **16b**). Strongly electron-donating, electron-neutral and electron-withdrawing substituents were investigated. Unsubstituted 3-phenyl was examined in **12a**, **13a**, **14a**, **15a**, **16a**. Weakly basic and neutral heterocycles (replacing the 3-phenyl) were incorporated in **13p**–**r**, **14h**, **15g**–**i**, some being electron-poor and some being electron-rich. The optimal location of the substituent on the 3-aryl ring was tested in five sets of compounds, **12b**,**c**, **12d**–**f**, **12g**–**i**, **12k**–**n** and **13f**–**h**. The effect of an *ortho*-substituent may be to twist the 3-aryl ring out of the plane of the isoquinolinone; this potential twist was replicated in **17** with a methyl group in the 4-position ('*ortho*' to the phenyl).

The preliminary SAR in the quinazolin-4-one series[36] and the crystal structures used here gave limited predictive information on the precise dimensions and the flexibility of the hydrophobic cavity; thus we tested these with the greater steric bulk of **12n**, **13c**,**i**,**q**, **15h** and, in extremis, by the ferrocene in **13s**. The dimensions were also tested by inserting a CH_2CH_2 spacer between the isoquinolinone and the phenyl ring in **12s**. The tunnel at the end of the hydrophobic cavity distal from the isoquinolinone-binding subsite would be occupied by a long rigid hydrophobic group in **13k**. This space was also explored in **13l**–**o**. The latter compounds incorporate a tertiary aliphatic amine to aid water-solubility; a protonated primary aliphatic amine in this position leads to major loss of activity in the quinazolin-4-ones[36] and an aniline may not be sufficiently basic for formation of soluble salts.

2.2. Chemical synthesis

5-AIQ **11a** (Fig. 1), has been prepared by a number of different routes, including Polonovski rearrangement of 5-nitroisoquinoline-*N*-oxide followed by reduction of the nitro group[56] and selective reduction of the nitrile of methyl 2-cyanomethyl-3-nitrobenzoate,[57] cyclisation in situ and further reduction. The current optimum method is condensation of methyl 2-methyl-3-nitrobenzoate with DMFDMA, hydrolysis of the enamine to 5-nitroisocoumarin, conversion to 5-nitroisoquinolin-1-one and reduction.[40] However, none of these routes can be adapted readily to the preparation of a library of 3-substituted analogues. We previously reported some approaches to the target compounds (Scheme 1) but each suffers from lack of generality and modest yield and none feature late introduction of the 3-substituent, a requirement for efficient preparation of a focussed library. Sonogashira coupling of methyl 2-iodo-3-nitrobenzoate **18** with phenylethyne, followed by 6-*endo*-dig cyclisation of the alkyne **19**, gave the isocoumarin **20** (R^3 = Ph),[58] leading to **22** (R^3 = Ph) and hence to **12a** (R^3 = Ph). Similar electrophilic cyclisation of **19** with ICl led to the isocoumarin **21** and hence to **20** (R^3 = Ph).[58] The initial Sonogashira reaction was limited to this example. Reaction of **23** with Cu(I) phenylacetylides under Castro–Stephens conditions gave the **17** directly but only when R^3 = Ph, 4-MePh and 4-MeOPh.[58] Hurtley couplings of the corresponding bromonitrobenzoic acid **24** afforded a wide range of intermediate isocoumarins **20** directly but the yields were modest and the reaction was limited to R^3 = alkyl, electron-rich aryl.[51] Nevertheless, samples of **12a**,**c**,**f**,**m** were prepared for this study. Finally, treatment of **25** with benzoyl chlorides under Friedel–Crafts conditions gave modest yields of **20** but this process failed for electron-donating substituents.[59] There was, therefore, a pressing need to design a synthetic route which allowed efficient late incorporation of diverse 3-substituents.

We have previously described Pd-catalysed Suzuki–Miyaura and Stille couplings to 1-alkoxy-4-bromo-5-nitroisoquinolines as a method to access 4-substituted analogues of 5-AIQ **11a**, which are inhibitors of PARP-2.[60] Adaptations of this method were explored to access the required corresponding 3-aryl-5-AIQs. 1,3-Dichloroisoquinoline **26** was nitrated selectively at the 5-position under highly acidic conditions to give **27** (Scheme 2). A methoxy group at the 1-position would serve as a masked lactam; the lactam in the target compounds is essential for biological activity but it also renders the isoquinolin-1-ones highly insoluble in organic solvents used for coupling reactions. This methoxy group was introduced using methoxide ion in methanol, giving **28**; this reaction is highly selective for displacement of the chlorine at

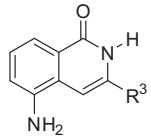

12: **a**: R^3 = Ph; **b**: R^3 = 3-MePh; **c**: R^3 = 4-MePh; **d**: R^3 = 2-MeOPh; **e**: R^3 = 3-MeOPh; **f**: R^3 = 4-MeOPh; **g**: R^3 = 2-F_3CPh; **h**: R^3 = 3-F_3CPh; **i**: R^3 = 4-F_3CPh; **j**: R^3 = 4-FPh; **k**: R^3 = 2-ClPh; **l**: R^3 = 3-ClPh; **m**: R^3 = 4-ClPh; **n**: R^3 = 2,6-Cl_2Ph; **o**: R^3 = 4-BrPh; **p**: R^3 = 4-HOPh; **q**: R^3 = 3-NCPh; **r**: R^3 = 4-NCPh; **s**: R^3 = PhCH_2CH_2; **t**: R^3 = 3-H_2NOCPh; **u**: R^3 = 4-H_2NOCPh

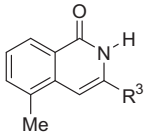

13: **a**: R^3 = Ph; **b**: R^3 = 4-MePh; **c**: R^3 = 4-Bu^{t}Ph; **d**: R^3 = 4-MeOPh; **e**: R^3 = 4-F_3CPh; **f**: R^3 = 2-ClPh; **g**: R^3 = 3-ClPh; **h**: R^3 = 4-ClPh; **i**: R^3 = 2,6-Cl_2Ph; **j**: R^3 = 4-BrPh; **k**: R^3 = 4-PhC≡CPh; **l**: R^3 = 4-Me_2NCH_2Ph; **m**: R^3 = 4-(piperidin-1-yl)CH_2Ph; **n**: R^3 = 4-(pyrrolidin-1-yl)CH_2Ph; **o**: R^3 = 4-(4-methylpiperazin-1-yl)CH_2Ph; **p**: R^3 = pyridin-4-yl; **q**: R^3 = benzo-1,3-dioxol-5-yl; **r**: R^3 = thiophen-3-yl; **s**: R^3 = ferrocenyl

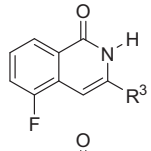

14: **a**: R^3 = Ph; **b**: R^3 = 4-MePh; **c**: R^3 = 4-MeOPh; **d**: R^3 = 4-F_3CPh; **e**: R^3 = 4-FPh; **f**: R^3 = 4-ClPh; **g**: R^3 = 4-BrPh; **h**: R^3 = pyridin-4-yl

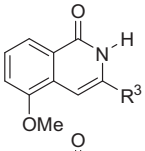

15: **a**: R^3 = Ph; **b**: R^3 = 4-MePh; **c**: R^3 = 4-Bu^{t}Ph; **d**: R^3 = 4-F_3CPh; **e**: R^3 = 4-ClPh; **f**: R^3 = 4-BrPh; **g**: R^3 = pyridin-4-yl; **h**: R^3 = benzo-1,3-dioxol-5-yl; **i**: R^3 = thiophen-3-yl

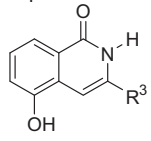

16: **a**: R^3 = Ph; **b**: R^3 = 4-F_3CPh

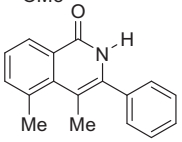

17

Figure 3. Structures of designed tankyrase-inhibiting isoquinolin-1-ones **12**–**17**.

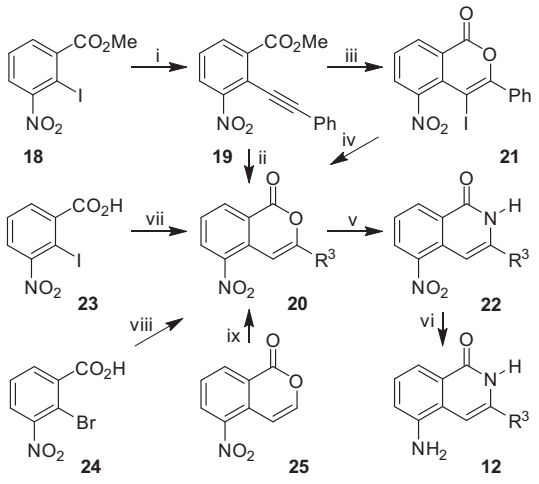

Scheme 1. Earlier synthetic routes explores to 3-substituted analogues **12** of 5-AIQ **11a**; R^3 = alkyl, aryl. Each of these suffers from poor yield or lack of generality or both. Reagents: (i) HC≡CPh, $(Ph_3P)_2PdCl_2$, Pr^i_2NH, THF; (ii) $HgSO_4$, H_2SO_4, Me_2CO, Δ; (iii) ICl, CH_2Cl_2; (iv) HCO_2H, $Pd(OAc)_2$, Et_3N, DMF; (v) NH_3, $MeOCH_2CH_2OH$, Δ; (vi) H_2, Pd/C, aq HCl, EtOH or $SnCl_2$, EtOH; (vii) CuC≡CR^3, pyridine, Δ (R^3 Ph, 4-MePh, 4-MeOPh); (viii) $(R^3CO)_2CH_2$ or R^3COCH_2COMe, Cu powder, $KOBu^t$, $HOBu^t$, Δ (R^3 = alkyl, electron-rich aryl); (ix) R^3COCl, $SnCl_4$, $PhNO_2$, Δ, (R^3 = electron-poor aryl).

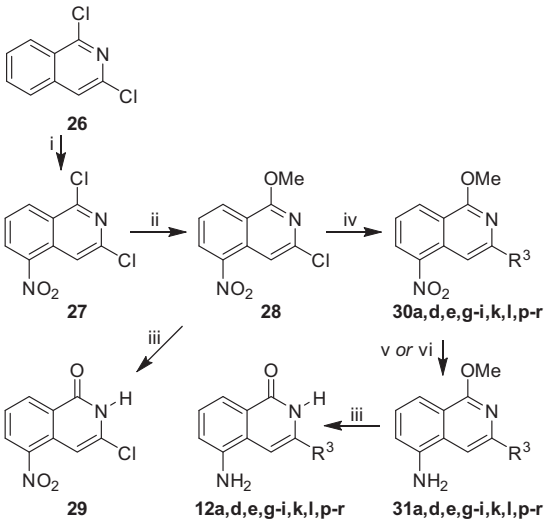

Scheme 2. Synthesis of target 5-amino-3-arylisoquinolin-1-ones **12a**,**d**,**e**,**g**–**i**,**k**,**l**,**p**–**r** via Suzuki–Miyaura couplings to 3-chloro-1-methoxy-5-nitroisoquinolin-1-one **28**. R^3 as for Figure 2. Reagents: (i) HNO_3, H_2SO_4; (ii) NaOMe, MeOH; (iii) HBr, AcOH; (iv) $R^3B(OH)_2$, Pd_2dba_3, SPhos, K_3PO_4, toluene (DMF for **28** → **30p**); (v) H_2, Pd/C, EtOH (**30a**,**d**,**e**,**g**–**i**,**p**–**r** → **31a**,**d**,**e**,**g**–**i**,**p**–**r**); (vi) H_2, Pt/C, EtOH (**30k**,**l** → **31k**,**l**).

the 1-position, with no reaction at the 3-position even under prolonged or more forcing conditions.

Pd-catalysed coupling of an appropriate 3-chloroisoquinolin-1-one would be desirable, as it places the point of introduction of diversity very late in the sequence, such that each coupled analogue only required one further step to generate the targets **12**. Demethylation of **28** with hydrogen bromide in acetic acid gave **29** in moderate yield (Scheme 2). However, this material was very poorly soluble in solvents appropriate for Suzuki–Miyaura couplings and all attempts to couple it with arylboronic acids failed.

By contrast, **28** (containing the lactam masked as the 1-methoxy group) had excellent solubility in common organic solvents. Coupling with arylboronic acids carrying simple substituents at *ortho*-, *meta*- or *para*-positions, using a Pd_2dba_3/SPhos combination in boiling toluene was moderately effective, giving **12a**,**d**,**e**,**g**–**i**,**k**,**l**,**p**–**r** in moderate yields. Varying amounts of unreacted **28** were recovered but the unreacted boronic acids decomposed under the reaction conditions. Repetition of the reactions with excess arylboronic acids, either from the start of the reaction or added portionwise during the procedure, failed to increase the yields. The yields of isolated 3-arylisoquinolines **30a**,**d**,**e**,**g**–**i**,**k**,**l**,**p**–**r** were also lowered by difficulties in separation of **30a**,**d**,**e**,**g**–**i**,**k**,**l**,**p**–**r** from **28**. Catalytic hydrogenation reduced the nitro groups of **30a**,**d**,**e**,**g**–**i**,**k**,**l**,**p**–**r** to the required amines in **31a**,**d**,**e**,**g**–**i**,**k**,**l**,**p**–**r**. Palladium on charcoal was a satisfactory catalyst for most of the reductions but the monochlorophenylisoquinolines **30k**,**l** also suffered reductive loss of the chlorine under these conditions (giving **31a**). This dehalogenation was suppressed by the use of platinum on charcoal as catalyst. Curiously, **30n** was not dehalogenated during formation of **31n**.

It was rationalised that increasing the reactivity of the 3-haloisoquinoline would have two benefits: (a) the intrinsic yield would be higher, (b) separation of starting isoquinoline from product isoquinolines would be easier, as less of the former would be present in the product mixture before chromatography. 1,3-Dibromoisoquinoline **34** is not commercially available at an economical price and had to be synthesised in two steps from inexpensive homophthalic acid **32** (Scheme 3). Heating **32** with urea at 180 °C in a solvent-free reaction gave the imide **33**. An attempt to replace both oxygens with bromines using phosphorus tribromide gave a modest yield of **34**, along with some of the deoxygenated side-product **35**. Clearly, the P(III) reagent is responsible for this side-reaction and analogous treatment with phosphorus oxybromide, gave only **34**. Nitration of **34** under highly acidic conditions afforded **36** in almost quantitative yield. As in the chloro series above, the 1-bromine could be replaced selectively with methoxide to give **37**, with no evidence of reaction at the 3-position despite the increased leaving-group ability of Br versus Cl. The regioisomeric identity of **37** was confirmed by a HMBC NMR experiment, with correlation between the OCH_3 protons and isoquinoline 1-*C* and by NOE correlation between OCH_3 and 8-*H*. The increased reactivity of the 3-bromoisoquinoline **37** led to more effective Suzuki–Miyaura couplings with a wide range of arylboronic acids to give **30**. As shown in Scheme 3, this coupling tolerated a variety of substituents on the boronic acid. Steric bulk generally lowered the yield but the 2,6-dichloro analogue **30n** was formed from **37**. Changing the reaction solvent to DMF and raising the reaction temperature to 135 °C raised the yields. Table 1 shows direct comparisons between the yields obtained in coupling using the 3-chloroisoquinoline **28** and the 3-bromoisoquinoline **37** as the haloarene component. In general, yields were improved with **37** and with DMF as reaction solvent. The highly reactive **37** also permitted coupling with 4-bromophenylboronic acid, without homo-coupling of the boronic acid. The poor solubility of 4-hydroxyphenylboronic acid in toluene led to very low yields for couplings in this solvent but DMF enabled preparation of **30p** in good yield from **28** and from **37**.

There are two possible sequences from **30** to the targets **12**, demethylation then reduction or vice versa. The former was investigated with three examples. Demethylation of **30a**,**i**,**j** with hydrogen bromide in acetic acid gave the corresponding 3-aryl-5-nitroisoquinolin-1-ones **22a**,**i**,**j** in good yields. However, the poor solubility of these nitroisoquinolin-1-ones in solvents appropriate for catalytic hydrogenation of the nitro groups precluded efficient conversion to **22a**,**i**,**j**. Thus **30g**–**n**,**p**–**r** were first reduced to **31g**–**n**,**p**–**r**, using hydrogen and Pd or Pt as appropriate (Pt was required for some examples to avoid reductive dehalogenation). Demethylation was effected with hydrogen bromide in

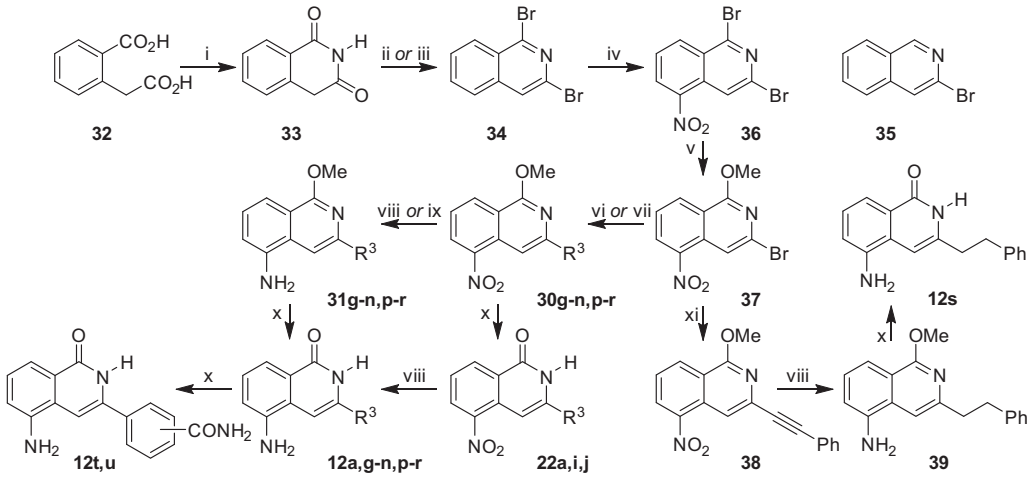

Scheme 3. Synthesis of target 3-substituted 5-aminoisoquinolin-1-ones **12a–g,n,p,t,u** via Suzuki–Miyaura and Sonogashira couplings to 3-bromo-1-methoxy-5-nitroisoquinoline **37**. R^3 as for Figure 2. Reagents: (i) urea, 180 °C, no solvent; (ii) PBr_3; (iii) $POBr_3$. 1,4-dioxan; (iv) HNO_3, H_2SO_4; (v) NaOMe, MeOH; (vi) $R^3B(OH)_2$, Pd_2dba_3, SPhos, K_3PO_4, toluene; (vii) $R^3B(OH)_2$, Pd_2dba_3, SPhos, K_3PO_4, DMF; (viii) H_2, Pd/C, EtOH; (ix) H_2, Pt/C, EtOH; (x) HBr, AcOH; (xi) PhC≡CH, $(Ph_3P)_2PdCl_2$, CuI, Na ascorbate, THF, Pr^i_2NH.

Table 1
Comparison of Suzuki–Miyaura coupling yields using 3-chloro-1-methoxy-5-nitroisoquinoline **28** and 3-bromo-1-methoxy-5-nitroisoquinoline **37**

Boronic acid	3-Aryl-1-MeO-5-O_2N-isoquinoline	Isolated yield from **28** (%)	Isolated yield from **37** (%)
2-F_3CPhB(OH)$_2$	**30g**	42[a]	42[b]
3-F_3CPhB(OH)$_2$	**30h**	55[a]	63[b]
4-FPhB(OH)$_2$	**30j**	0[a]	40[b]
2-ClPhB(OH)$_2$	**30k**	100[a]	60[b]
3-ClPhB(OH)$_2$	**30l**	34[a]	52[b]
4-BrPhB(OH)$_2$	**30o**	0[a]	24[b]
4-HOPhB(OH)$_2$	**30p**	0[a], 64[b]	9[a], 86[b]
3-NCPhB(OH)$_2$	**30q**	8[a]	12[b]
4-NCPhB(OH)$_2$	**30r**	28[a]	12[b]

[a] Reaction solvent toluene, 110 °C.
[b] Reaction solvent DMF, 135 °C.

acetic acid, a medium in which the 5-aminoisoquinolines were readily soluble, to furnish the required **12g–n,p–r** in good yields as their HBr salts. There was no evidence of demethylation of the 4′-methoxy group in **31f**, indicating the selectivity of the conditions chosen. The nitriles in **31q,r** were hydrated under these vigorous conditions to give the carboxamides **12t,u**, rather than **12q,r**.

Sonogashira coupling of phenylethyne to the 3-bromoisoquinoline **37** was also high yielding, giving the 3-phenylethynyl analogue **38**. The nitro group of **38** could not be reduced selectively but catalytic hydrogenation provided **39**. Demethylation afforded **12s** as the hydrobromide salt.

The 5-methyl-, 5-fluoro-, 5-methoxy- and 5-hydroxy-3-arylisoquinolin-1-ones **13a–s**, **14a–h**, **15a–i** and **16a,b** were prepared by a different route (Scheme 4). Poindexter described a route to simple 3-arylisoquinolin-1-ones by double deprotonation of *N*,2-dimethylbenzamide with butyllithium and reaction with benzonitriles.[61] Cho et al. extended this method to removal of a proton from the Ar-CH_3 of the tertiary amide *N*,*N*,2-trimethylbenzamide with lithium diisopropylamide at −78 °C and subsequent reaction with benzonitriles lacking acidic functional groups.[62] We have extended this process to the synthesis of 3-aryl-5-substituted-isoquinolin-1-ones from *N*,*N*,2,3-tetramethylbenzamide **41**, 3-fluoro-*N*,*N*,2-trimethylbenzamide **49** and 3-methoxy-*N*,*N*,2-trimethylbenzamide **51**. The advantage of this route is that the diversity in the 3-aryl substituent is introduced at the final stage of the synthesis, through diversity in the benzonitriles.

2,3-Dimethylbenzoic acid **40** was converted into its *N*,*N*-dimethylamide **41** in the usual way. Treatment with one equivalent of LDA in THF at −78 °C selectively removed a proton from the 2-CH_3. The anion reacted with a range of benzonitriles to provide the corresponding 3-aryl-5-methylisoquinolin-1-ones **13a–j** in poor-to-excellent yields. The lower yields were due not to failure of reaction but to issues in isolation of these compounds which are of limited solubility in convenient organic solvents; sufficient material was obtained in each case for biochemical evaluation. The reaction was sensitive to steric crowding in the benzonitrile, with 2-chlorobenzonitrile and 2,6-dichlorobenzonitrile giving low yields of **13f,i**, respectively. No transmetalation was seen with 4-bromobenzonitrile, which gave a satisfactory yield of **13j**. The reaction was also applicable to heterocyclic nitriles, with 4-cyanopyridine, 5-cyanobenzo-1,3-dioxole and 3-cyanothiophene reacting well with the anion derived from **41** to give the 3-heteroaryl-5-methylisoquinolin-1-ones **13p–r**.

Isoquinolin-1-ones **13k–o** carry extensions at the 4′-position of the 3-phenyl substituent either to probe the far side of the hydrophobic pocket or to elicit solubility in water but the corresponding benzonitriles **43**,**45a–d** are not commercially available. Sonogashira coupling of 4-bromobenzonitrile **42** with phenylethyne gave 4-phenylethynylbenzonitrile **43** in good yield. The 4-(aminomethyl)benzonitriles **45a–d** were prepared from 4-bromomethylbenzonitrile **44** and secondary amines, under a variety of basic conditions (Scheme 4). These benzonitriles gave the corresponding isoquinolinones **13k–o**. These analogues **13l–o** were converted to their hydrochloride salts, which showed much-enhanced aqueous solubility. The 3-ferrocenylisoquinolinone target **13s** tests whether the hydrophobic pocket could accommodate three-dimensional steric bulk while still retaining aromaticity, rather than the planar aromatic 3-substituents of **13a–r**. Commercially available ferrocenecarboxylic acid **46** was converted into its carboxamide, which was dehydrated into the nitrile **47** in high yield. Reaction with the anion of **41** proceeded in moderate yield to give **10s**, despite the steric bulk of the ferrocene.

This one-step assembly of 3-aryl-5-substituted isoquinolin-1-ones was extended into the 5-fluoro analogues **14a–h** and the 5-methoxy compounds **15a–i** (Scheme 4). 3-Fluoro-3-methylbenzoic acid **48** and 3-methoxy-2-methylbenzoic acid **50** were readily converted into the corresponding *N*,*N*-dimethylbenzamides **49**, **51**, respectively, via the acid chlorides. Again, the derived anions reacted smoothly with a range of benzonitriles to give **14a–h** and

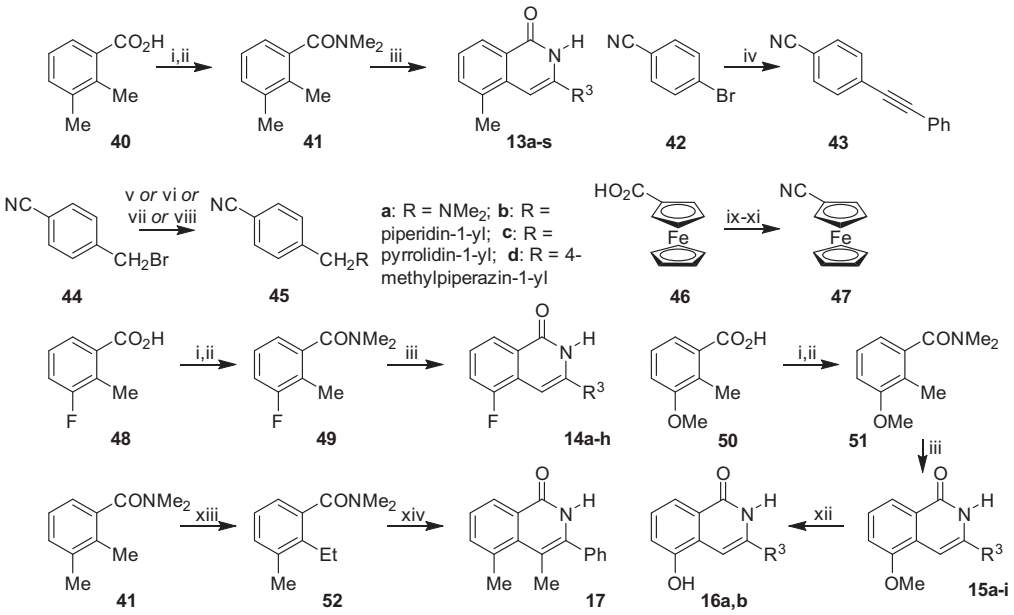

Scheme 4. Syntheses of 3-aryl-5-methylisoquinolin-1-ones **13**, 3-aryl-5-fluoroisoquinolin-1-ones **14**, 3-aryl-5-methoxyisoquinolin-1-ones **15**, 3-aryl-5-hydroxyisoquinolin-1-ones **16** and 4,5-dimethyl-3-phenylisoquinolin-1-one **17**. Reagents: (i) $SOCl_2$; (ii) aq, Me_2NH, CH_2Cl_2; (iii) $LiNPr^i_2$, R^3CN, THF, −78 °C; (iv) $PhC{\equiv}CH$, $(Ph_3P)_2PdCl_2$, CuI, Na ascorbate, Pr^i_2NH, THF; (v) aq Me_2NH; (vi) piperidine, K_2CO_3, DMF; (vii) pyrrolidine, Et_3N, THF; (viii) 1-methylpiperazine, Et_3N, CH_2Cl_2; (ix) $(COCl)_2$; (x) NH_3, Et_2O; (xi) $POCl_3$, Δ; (xii) BBr_3, CH_2Cl_2; (xiii) $LiNPr^i_2$, MeI, THF, −78 °C; (xiv) *sec*-BuLi, R^3CN, THF, −78 °C.

15a–i, confirming that neither the deprotonation of the Ar-CH_3 nor the subsequent attack of the carbanion on the nitrile and cyclisation were adversely affected by the electron-withdrawing fluorine or the electron-donating methoxy group *ortho* to the methyl. Two examples **15a**,**d** were demethylated at the 5-position to provide the corresponding 5-hydroxyisoquinolin-1-one **16a**,**b** using boron tribromide.

4-Alkylisoquinolin-1-ones have been prepared by Stille coupling of 4-bromo-1-methoxyisoquinolines[60] and by Pd-catalysed double-bond migration and cyclisation of *N*-allyl-2-halobenzamides.[52] However, neither of these methods provides a short access to 4,5-dimethyl-3-phenylisoquinolin-1-one **17**. This target was approached by twice exploiting the nucleophilic reactivity of the CH_2-carbanion *ortho* to the lithium-coordinating dimethylamide. *N*,*N*,2,3-Tetramethylbenzamide **41** was deprotonated selectively at the 2-CH_3 and reaction with iodomethane gave the 2-ethyl analogue **52**. However, treatment of **52** with lithium diisopropylamide failed to give the corresponding $ArC^{(-)}HMe$ anion, as shown by the lack of incorporation of deuterium upon quench with deuterium oxide. The stronger base, *sec*-butyllithium, was successful in removing one of the methylene protons and reaction of the anion with benzonitrile gave **17**, demonstrating that this synthesis of isoquinolin-1-ones is applicable to 4-alkyl analogues.

2.3. Biochemical evaluation

Target compounds were initially screened for inhibition of the activity of TNKS-2 at 1.0 μM, 100 nM and 10 nM using immobilised truncated human TNKS-2 containing the catalytic (NAD^+-binding) and adjacent sterile α-motif (SAM) domains. This assay measures autopoly(ADP-ribosyl)ation of the enzyme with a mixture of NAD^+ and biotin-labelled NAD^+; the biotinylated poly(ADP-ribose) is then quantified with streptavidin-horseradish peroxidase.[36] The data are shown in Table 2. IC_{50} values were then determined for examples selected for potency at 10 nM and which would give detailed information about the structural requirements for activity (Table 2). Many selected compounds were also evaluated for inhibition of full-length human TNKS-1 (using immobilised histones as co-substrate) and counter-screened against human PARP-1[36] and murine or human PARP-2 to assess selectivity (Table 2). The PARP-1 assays were conducted using a commercial kit; PARP-2 assays were conducted for **11a**, **12a**,**f**,**i**,**m** with murine PARP-2 as described previously[63] and for **13b**,**k**,**p**, **14b**, **15b** with human PARP-2 using a commercial kit.

2.4. Structure–activity relationships

2.4.1. Structure–activity relationships—5-position

Examining the data for inhibition of TNKS-2 (Table 2), a trend is evident for the 5-substituent. Comparing the six analogues **12i**, **13e**, **14d**, **15d**, **16b**, **22i** where the 3-substituent is kept constant as 4-trifluoromethylphenyl, potency increases in the order 5-F < 5-NO_2 = 5-OH < 5-NH_2 < 5-Me = OMe. This trend is also observed for the entire set of 3-arylisoquinolinones. The data suggest that an electron-donating or electron-neutral hydrophobic group is optimum at this 5-position, with the electron-withdrawing fluorine and nitro groups having diminished activity. Similarly, H-bond donors (hydroxy, amino) reduce the inhibitory potency and hydrophobic groups (methyl, methoxy) are preferred. Finally, modest size improves activity, with the 5-fluoro compounds showing lower potency; C–F occupies similar steric space as does C–H. Interestingly, this correlates with the observed preference for 8-methyl and 8-methoxy in the 2-arylquinazolin-4-one series (corresponding to the 5-position in isoquinolinones), where the 5-H compound was significantly less active.[36] This trend can be rationalised structurally by considering that the space available to this 5-substituent is expected to be that occupied by the ribose anomeric carbon and adjacent 2′-CHOH and ether oxygen when NAD^+ is bound. The part of this space immediately adjacent to the isoquinolinone 5-carbon is of mixed hydrophilic and hydrophobic character, being bounded by an edge of the aromatic ring and the CH_2 of Tyr^{1050}, an edge of the aromatic ring of Tyr^{1060}, the ε-CH_2 of Lys^{1067} and the OH of Tyr^{1071}. Further away from the

Table 2
Inhibition of the catalytic activities of TNKS-2, TNKS-1, PARP-1 and PARP-2 by isoquinolin-1-ones **11**–**17**, **22** and by positive control **1**

Compd no.	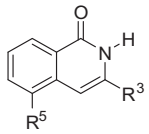		TNKS-2				TNKS-1 IC_{50} (nM)	PARP-1 IC_{50} (nM)	PARP-2 IC_{50} (nM)
	R^3	R^5	% inhibition (1.0 μM)	% inhibition (100 nM)	% inhibition (10 nM)	IC_{50} (nM)			
1	—	—	97 ± 10	87 ± 10	53 ± 2	15 ± 3	15 ± 4	[a]	
11a	H	NH_2	16 ± 8	18 ± 7	9 ± 20			1600 ± 250[b]	1050 ± 150[b,d]
12a	Ph	NH_2	92 ± 2	60 ± 8	18 ± 1			1070 ± 70[b]	480 ± 150[b,d]
12c	4-MePh	NH_2	100 ± 8	100 ± 2	84 ± 4	34 ± 14	39	880 ± 140[b]	
12d	2-MeOPh	NH_2	48 ± 10	0 ± 12	21 ± 17				
12e	3-MeOPh	NH_2	76 ± 12	54 ± 14	11 ± 18				
12f	4-MeOPh	NH_2	73 ± 16	41 ± 2	0 ± 26			900 ± 210[b]	730 ± 250[b,d]
12g	2-F_3CPh	NH_2	1 ± 10	8 ± 27	15 ± 20				
12h	3-F_3CPh	NH_2	82 ± 1	33 ± 6	27 ± 6				
12i	4-F_3CPh	NH_2	100 ± 1	97 ± 2	60 ± 1			330 ± 70[b]	170 ± 20[b,d]
12j	4-FPh	NH_2	100 ± 2	85 ± 4	55 ± 1				
12k	2-ClPh	NH_2	40 ± 7	15 ± 7	10 ± 12				
12l	3-ClPh	NH_2	89 ± 2	57 ± 4	36 ± 6				
12m	4-ClPh	NH_2	94 ± 2	88 ± 0	65 ± 4			570 ± 30[b]	160 ± 50[b,d]
12n	2,6-Cl_2Ph	NH_2	4 ± 4	0 ± 29	8 ± 15				
12p	4-HOPh	NH_2	100 ± 4	100 ± 8	58 ± 10				
12s	$PhCH_2CH_2$	NH_2	78 ± 8	38 ± 22	20 ± 12				
12t	3-H_2NOCPh	NH_2	20 ± 7	11 ± 32	32 ± 19				
12u	4-H_2NOCPh	NH_2	100 ± 1	92 ± 5	80 ± 8				
13a	Ph	Me	100 ± 2	94 ± 3	86 ± 3	1.8 ± 0.1			
13b	4-MePh	Me	100 ± 0	100 ± 2	100 ± 1	1.3 ± 0.5	21 ± 3	>10,000[c]	>10,000[e]
13c	4-Bu^{t}Ph	Me	91 ± 34	88 ± 18	78 ± 12	5.7 ± 2.0			
13d	4-MeOPh	Me	100 ± 5	100 ± 15	90 ± 5	1.6 ± 0.2			
13e	4-F_3CPh	Me	100 ± 1	100 ± 1	98 ± 1	9 ± 4	43 ± 6	1400 ± 450	
13f	2-ClPh	Me	87 ± 7	17 ± 12	0 ± 14				
13g	3-ClPh	Me	95 ± 10	81 ± 2	22 ± 24	91 ± 60	181 ± 21	>10,000[c]	
13h	4-ClPh	Me	98 ± 2	88 ± 7	70 ± 6	32 ± 25	275 ± 32	>10,000[c]	
13i	2,6-Cl_2Ph	Me	0 ± 21	1 ± 26	5 ± 5	836 ± 95	1340	>5000[c]	
13j	4-BrPh	Me	95 ± 26	100 ± 10	88 ± 12	20 ± 1			
13k	4-PhC≡CPh	Me	100 ± 10	100 ± 2	71 ± 25	9.6 ± 3.6	>1000	>10,000[c]	>10,000[e]
13l	4-Me_2NCH_2Ph	Me	100 ± 9	100 ± 20	70± 3				
13m	4-(Piperidin-1-yl)CH_2Ph	Me	100 ± 29	100 ± 11	61 ± 3	9.8 ± 5.1			
13n	4-(Pyrrolidin-1-yl)CH_2Ph	Me	60 ± 12	41 ± 12	0 ± 14	1200 ± 210	$12 \times 10^3 \pm 2 \times 10^3$	>10,000[c]	
13o	4-(4-Me-piperazin-1-yl)CH_2Ph	Me	100 ± 6	79 ± 12	61 ± 8				
13p	Pyridin-4-yl	Me	100 ± 9	100 ± 16	20 ± 20	29 ± 4	48 ± 26	111 ± 23	163 ± 67[e]
13q	Benzodioxol-5-yl	Me	95 ± 10	98 ± 11	51 ± 17				
13r	Thiophen-3-yl	Me	87 ± 17	77 ± 5	49 ± 15	19 ± 4	74 ± 27	720 ± 230	
13s	Ferrocenyl	Me	67 ± 10	54 ± 10	0 ± 1				
14a	Ph	F	100 ± 3	100 ± 10	87 ± 12	23 ± 5			
14b	4-MePh	F	95 ± 8	91 ± 5	54 ± 5	3.8 ± 0.5	64 ± 3	>10,000[c]	>10,000[e]
14c	4-MeOPh	F	98 ± 19	98 ± 7	66 ± 14				
14d	4-F_3CPh	F	100 ± 11	79 ± 8	21 ± 17				
14f	4-ClPh	F	100 ± 17	100 ± 22	83 ± 17	11 ± 2			
14g	4-BrPh	F	73 ± 7	92 ± 7	73 ± 5				
14h	Pyridin-4-yl	F	29 ± 17	26 ± 12	15 ± 5				
15a	Ph	OMe	100 ± 2	100 ± 13	88 ± 5	28 ± 0.6			
15b	4-MePh	OMe	100 ± 17	100 ± 20	100 ± 2	5.1 ± 0.6	30 ± 14	>10,000[c]	>10,000[e]
15c	4-Bu^{t}Ph	OMe	100 ± 4	90 ± 12	74 ± 8	3.8 ± 1.2			
15d	4-F_3CPh	OMe	100 ± 25	100 ± 2	100 ± 14	2.5 ± 0.9			
15e	4-ClPh	OMe	100 ± 12	100 ± 15	100 ± 10	5.5 ± 0.3			
15f	4-BrPh	OMe	76 ± 8	65 ± 2	58 ± 5				
15g	Pyridin-4-yl	OMe	73 ± 17	50 ± 27	14 ± 2				
15h	Benzodioxol-5-yl	OMe	91 ± 26	87 ± 8	57 ± 15				
15i	Thiophen-3-yl	OMe	94 ± 10	73 ± 9	53 ± 4				
16a	Ph	OH	100 ± 0.5	86 ± 5	59 ± 9				
16b	4-F_3CPh	OH	85 ± 5	69 ± 5	50 ± 9				
17	Ph	Me[f]	100 ± 4	90 ± 32	68 ± 16	19 ± 4	244	860 ± 210	
22i	4-F_3CPh	NO_2	93 ± 13	72 ± 9	44 ± 27				
22j	4-FPh	NO_2	47 ± 32	70 ± 19	55 ± 14				

[a] Table cells without data indicate Not Determined.
[b] Data taken from Ref. 44.
[c] Limited by solubility.
[d] Murine PARP-2.
[e] Human PARP-2.
[f] Also 4-Me.

isoquinolinones, the space becomes more polar, with the carboxylate of Glu[1138] and the ammonium of Lys[1067].

2.4.2. Structure–activity relationships—exploration of the hydrophobic cavity

Comparison of **11a** with the 3-phenyl analogue **12a** shows the need for a 3-aryl group. The nature and substitution of this group have a major role in determining potency, according to whether or not the substituted aryl can be accommodated in the hydrophobic cavity. The 3-(unsubstituted-phenyl)isoquinolinones **12a**, **13a**, **14a**, **15a**, **16a** all have good potency, taking into account the effect of the nature of the 5-substituent. The location of the groups attached to the 3-phenyl is seen to have a profound effect on binding. Within the isomeric set of 5-amino-3-(methoxyphenyl) isoquinolin-1-ones **12d**–**f**, the methoxy substituent appears to be moderately well tolerated at the *meta*- and *para*-positions of the 3-phenyl (in **12e**,**f**) but not at the *ortho*-position, leading to inactivity of **12d** below micromolar concentrations. A similar strong trend is seen for the corresponding isomeric set of 5-amino-3-(chlorophenyl)isoquinolin-1-ones **12k**–**m** but the *para*-chlorophenyl compound **12m** also appears to be marginally more active than the *meta*-analogue **12l**. Compound **12n**, with chlorines in both *ortho*-positions, is completely inactive. The same trend is also strongly evident in moving to the 5-methyl series, in that the *para*-chloro compound **13h** is very potent, the *meta*-chloro isomer **13g** is marginally less potent, with even lower activity for the *ortho*-chloro isomer **13f**. Again, the 2′,6′-dichloro analogue **13i** completely lacks activity. Thus the trend for optimum location of substituents on the 3-phenyl ring appears to be 4′ > 3′ ≫ 2′ >>> 2′,6′. We also observed this preference for flavones.[39] Interestingly, the benzo-1,3-dioxoles **13q** and **15h** retain activity; these can be considered as having the 3-phenyl rings disubstituted at the *meta*- and *para*-positions.

There are two possible structural rationalisations for this trend. Firstly, the hydrophobic cavity may simply be limited in size and flexibility at the end nearer the isoquinolinone-binding motif and thus not be able to accommodate bulky *ortho*-substituents. In this rationalisation, the hydrophobic cavity is larger and/or more flexible at the distal end, near the tunnel to the exterior, to accommodate substituents in the *meta*- and *para*-positions. In an alternative rationalisation, it may be the dihedral (twist) angle between the phenyl and the isoquinoline rings that controls binding in the hydrophobic cavity. The phenyl–isoquinoline system is essentially a biphenyl-like structure and the two rings may twist dihedrally about the linking bond to avoid steric clashes between 2-H and 4-H on the isoquinoline and 2′-H and 6′-H on the phenyl. Of course, if any of these positions were occupied by a bulky substituent, the propensity to twist out of the mutual plane would be greater. In this rationalisation, the hydrophobic cavity may be oval in cross-section and rigid, allowing the phenyl ring to bind in one plane but not in others. Resolution of this dichotomy is achieved by inducing the dihedral twist between the rings without the *ortho*-substituents on the phenyl; **17** has a methyl at the 4-position on the isoquinoline, which should induce the twist to avoid steric clash with 2′-H and 6′-H on the phenyl.

Small-molecule crystal structures were determined for **13i** (carrying a 2′,6′-dichlorophenyl) and for **15b**, which carries only a *para*-methylphenyl (Fig. 4). In **13i**, the two chlorines force a twist of 67° between the rings, whereas the rings are almost coplanar in **15b**, with a dihedral angle of only 1°. Unfortunately, the strict analogue **13h** did not form crystals of sufficient quality for X-ray diffraction. Molecular modelling of **13h** and **13i** bound into the nicotinamide-binding pocket and the hydrophobic cavity of TNKS-2 showed dihedral angles between the rings for **13h** (5°) and for **13i** (60°) in minimised structures (Fig. 5). The dihedral angles correlate with potency against the activity of the enzyme. Compound **17**, in which dihedral twist between the rings should be induced by the 4-Me, did not form crystals of suitable quality for small-molecule X-ray structure determination. However, when soaked into the crystal of TNKS-2, it bound well and a crystal structure was determined (Fig. 6). Similarly, a crystal structure was obtained for **15e** bound into TNKS-2 (Fig. 6). These crystal structures show that the rings are effectively coplanar in **15e**, whereas the aromatic rings are significantly twisted relative to each other in **17**. Thus the inhibitory activity towards TNKS-2 does not correlate well with the dihedral twist angle between the phenyl and isoquinoline rings, as **17** is only nine-fold less potent than **13a**. Loss of inhibitory activity does, however, correlate with the presence of bulky *ortho*-substituents on the phenyl ring. Compounds **12d**,**k**, **13f** with only one *ortho*-substituent on the 3-phenyl retain limited activity at 1.0 μM, whereas those with both *ortho*-positions occupied by bulky substituents (**12n**, **13i**) are completely inactive. This effect can be rationalised by considering **12d**,**k**, **10f** as existing as pairs of interconverting enantiomeric atropisomers, only one of which will bind to the enzyme, with the single *ortho*-substituent orientated away from steric clash with the protein. If there are two *ortho*-substituents, this is not possible and the compound cannot bind.

It can be seen that the optimum location for a substituent is the 4′-position, where it can interact with residues lining the hydrophobic cavity and/or project into the narrow tunnel. Accordingly, the size and nature of the 4′-substituent was studied. Across all series, several trends are evident. Particularly in **12** and **13**, the 4′-unsubstituted compound is slightly less active, so a substituent is preferred. Small lipophilic and polar substituents are tolerated equally, the former illustrated by **12c**,**i**, **13b**,**d**,**e**,**h**, **14b**–**d**,**f**, **15b**,**d**,**e** and the latter by **12p**,**u**. Interestingly this was not observed for 5-unsubstituted 3-arylisoquinolin-1-ones, implying differences between the scaffolds.[37] The electronic characteristics of the 4′-substituent also appear to be unimportant, comparing electron-donating (−I, +M) groups (**12f**,**p**, **13d**, **14c**, **15h**) with electron-withdrawing groups (−I: **12i**, **13e**, **14d**, **15d**, **16b**; −M: **12u**) and groups with approximately neutral electron-demand (**12c**,**m**, **13b**,**h**,**j**, **14b**,**f**,**g**, **15b**,**e**,**f**).

Thiophene and pyridine were also investigated as aromatic heterocyclic replacements for the 3-(substituted)phenyl ring. The thiophene in **13r**, **15i** maintains the activity, relative to the 3-phenyl parents **12a**, **15a**, respectively, as expected for this conservative replacement. However, the isosteric replacement with pyridine in **13p**, **14h**, **15g** produced some striking effects. Potency against TNKS-2 was dramatically reduced in **14h**, **15g**, whereas it was diminished slightly in **12p**. However, **12p** also inhibited the activity of PARP-1 strongly (IC_{50} = 111 nM), in contrast to most of the 3-(substituted)phenyl analogues counter-screened against this isoform and found to have low potency (IC_{50} = 860 nM to >10,000 nM).

The 3-aryl substituent was extended to test the boundaries and flexibility of the hydrophobic cavity and to explore the tunnel at the distal end. Firstly, a short flexible linker (–CH_2CH_2–) was interposed between the isoquinoline and the phenyl ring, taking the phenyl out of conjugation and pushing it towards the distal end of the cavity; this caused a marked loss of activity in **12s**. Secondly, diminution in activity was also caused by replacing simple planar aryl groups at the 3-position with the 3D bulk of

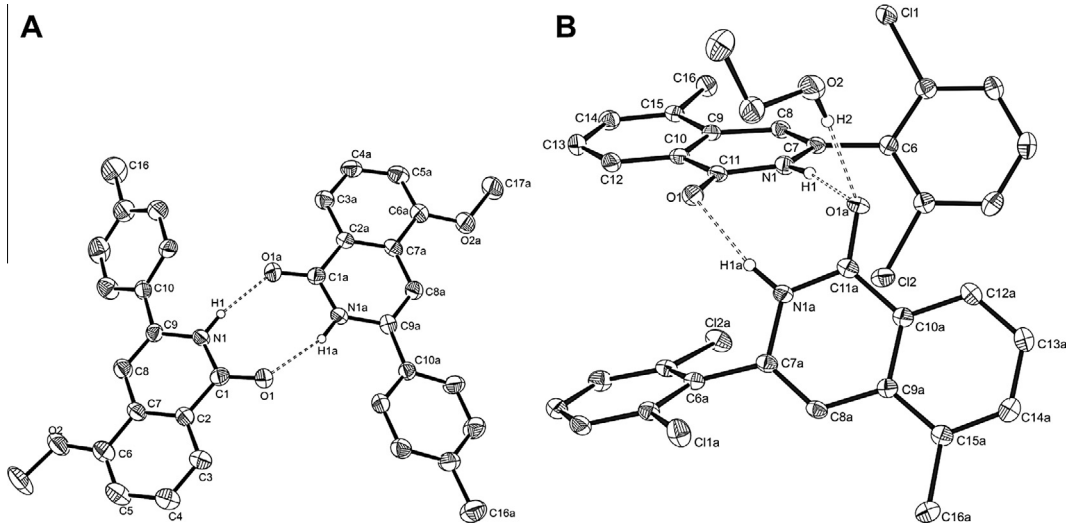

Figure 4. Crystal structures of **15b** (A) and **13i** (B). Ellipsoids are represented at 30% probability and only those hydrogens involved in H-bonding are shown for clarity. The structures show dihedral angles between the rings of 1° (**15b**) and 67° (**13i**).

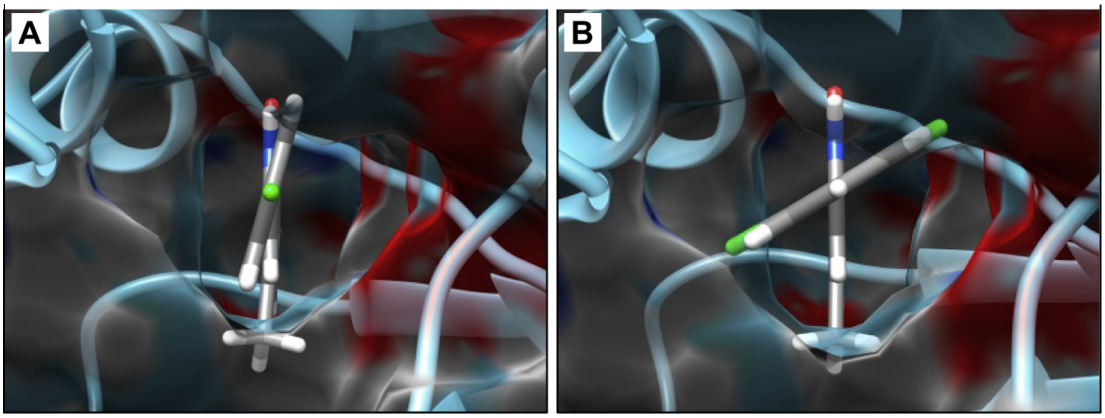

Figure 5. Minimised molecular models generated for **13h** (A) and **13i** (B) bound into the nicotinamide-binding pocket and adjacent hydrophobic cavity of tankyrase-2. The calculated dihedral angles between the rings are 60° (**13i**) and 5° (**13h**).

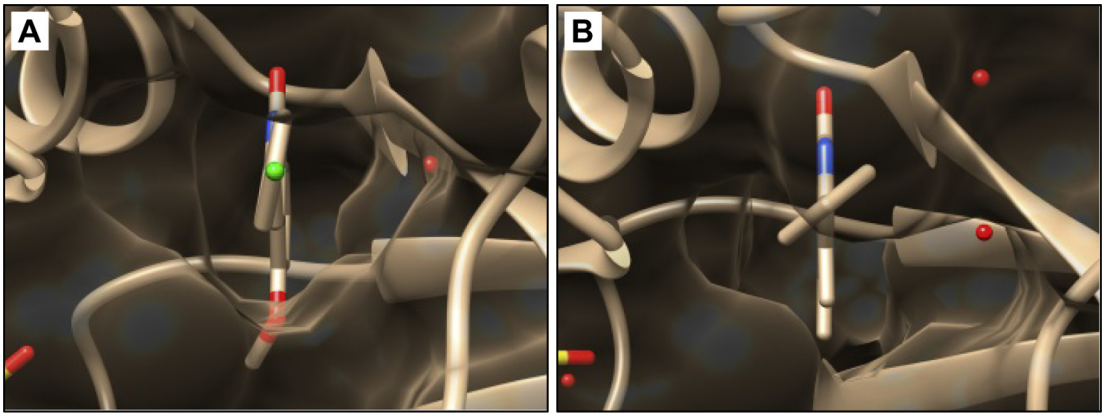

Figure 6. (A) Detail of crystal structure of **15e** in complex with tankyrase-2. (B) Detail of crystal structure of **17** in complex with tankyrase-2. The dihedral angle between the rings is 8° for **15e** and 50° for **17**.

ferrocene in **13s**. As with the mono-*ortho*-substituted phenyl compounds **12d**,**g**,**k**, **13f**, **13s** can exist as a pair of interconverting enantiomeric atropisomers and it is again likely that only one atropisomer can bind.

2.4.3. Structure–activity relationships—entering the tunnel

The tunnel at the distal end of the cavity was probed with the rigid hydrophobic 4′-phenylethynyl extension in **13k**. Modelling suggested that this group should occupy the whole tunnel, with

the distal phenyl starting to project into solvent. This compound was potent against TNKS-2, showing that the tunnel is directly aligned with the 4′-position on the proximal benzene ring and can accept a long narrow hydrophobic group.

The tunnel was also exploited in designing more water-soluble analogues. The isoquinolin-1-one pharmacophore usually gives high-melting solids of low aqueous solubility. A previous attempt to introduce a water-solubilising basic aliphatic amine to the 2-phenylquinazolin-4-one core with a 4′-$H_3N^+CH_2$ but abolished inhibitory activity against the TNKSs.[36] Modelling suggested that this primary ammonium would have to be accommodated in the hydrophobic part of the tunnel, giving unfavorable interactions. Thus, in the isoquinolinone series, tertiary aliphatic amines were incorporated at the corresponding 4′-position on the 3-phenyl ring, to provide a solubilising salt but without compromising lipophilicity severely. (Protonated)-4′-dimethylaminomethyl- (**13l**), 4′-(piperidin-1-yl)methyl- (**13m**) and 4′-(4-methylpiperazinyl) methyl- (**13o**) groups were accepted without major loss of activity but, curiously, the 4′-(pyrrolidin-1-yl)methyl analogue **13n** had very poor potency (IC_{50} = 1.2 μM). The HCl salts of **13l–o** were soluble to >2.5 mg mL^{-1} in water.

Table 2 also shows the activities of selected compounds against TNKS-1 and the results of counter-screening against PARP-1 and PARP-2. In general, the IC_{50} values against TNKS-1 parallel those found for TNKS-2. Most compounds were apparently more active against TNKS-2 than they were against the TNKS-1 isoform, an effect also seen in the preliminary studies with 2-aryl-8-methylquinazolin-4-ones,[36] but the assays use different constructs of the enzyme and different formats, so detailed comparisons must be made with caution. Worthy of note, however, is the apparent extreme selectivity of **13k** for inhibiting TNKS-2 (IC_{50} = 10 nM), whereas no inhibition of the activity of TNKS-1 is seen up to 1.0 μM. Most compounds examined were very poor inhibitors of PARP-1, with many IC_{50} values exceeding the limits of solubility at 5.0–10 μM. These data demonstrate that selectivity for TNKS-2 versus the PARP-1 isoform of up to 2.5×10^3—fold can be achieved (e.g., **14b**). Selected compounds were also counter-screened against another PARP isoform, PARP-2. The 5-amino-3-arylisoquinolin-1-ones **12a**,**f**,**i**,**m** inhibited PARP-2 moderately with IC_{50} values parallelling those for inhibition of PARP-1. By contrast, the 5-methyl-, 5-fluoro- and 5-methoxy-3-arylisoquinolin-1-ones **13b**,**k** **14b**,**15b** did not inhibit PARP-2 activity up to 10 mM. The major exception to this poor inhibition of PARP-1 and PARP-2 is the 3-(pyridin-4-yl) compound **13p**, which is essentially non-selective between the four isoforms examined and may constitute a new structural lead for inhibition of PARP-1/2.

2.5. Crystallographic studies on mode of binding

Protein crystallography was used during the studies to understand the modes of binding of the compounds to TNKSs. The catalytic domain of TNKS-2 was used in the structural studies and the structures were solved at 1.6–2.2 Å resolution. The asymmetric unit of the crystals contained two protein chains, which are almost identical at the compound-binding site. We will, therefore, only discuss chain A of the crystal structures. Importantly, the catalytic domains of TNKS-1 and TNKS-2 are highly homologous and the residues surrounding the binding sites are completely conserved.[67] The apo crystal structures of the proteins have differences in the conformations of the D-loops lining the substrate-binding site, which could indicate differences in dynamics of the proteins but may naturally also be caused by the crystal packing.[33] The current structural information does not explain the observed selectivity of **13k** between the isoforms of TNKS.

In total, twelve crystal structures were solved, including those of the small initial hit molecules **11a–d** (PDB codes 4UVL, 4UVP, 4UVS, 4UVT, respectively) in TNKS-2, establishing the initial mode of binding of the core scaffold, as described above. The improved analogue structures **12a**,**f**,**m**, **13h**,**n**, **14f**, **15e** and **17** (PDB codes 4UVZ, 4UVO, 4UVN, 4UVV, 4UVU, 4UVX, 4UVY, 4UVW, respectively) with varied 3- and 5-substituents were used to rationalise the SARs.

The compounds bind to the nicotinamide-binding site in the fashion expected for a typical inhibitor of PARPs. They make the canonical H-bonds with Gly^{1032} and Ser^{1068} of TNKS-2 (Fig. 7a), as well as π-stacking with Tyr^{1071}. Superposition of the protein structures reveals that the ligands occupy the same cavity in all the cases and the isoquinolinone moiety is nearly identically positioned in each case. Small structural changes in the surrounding residues induced by the binding of the analogues can be detected, when the crystal structures are compared. No structural changes were observed when the structures were compared with the TNKS-2 structure with nicotinamide bound (PDB code 3U9H).[49]

The initial small inhibitors **11a–d** bind very similarly, with no structural changes in the protein. Binding of the aryl group in the larger derivatives **12–15**, **17** causes Pro^{1034} and Phe^{1035} to move towards the hydrophobic extensions of the compounds (Fig. 7b). This induced fit is driven by the enhanced hydrophobic interaction of the closer fit of the compound. This change was not observed when a bulkier compound, **13n**, was bound to the active site. The long pyrrolidinyl extension towards the solvent is not well ordered in the crystal structure and the compound also has a lowered potency (Fig. 7a, Table 2). This contrasts with the retained activity of **13m** and **13o**. The dimethylaminomethyl group in **13l** does not extend to the solvent region with a hydrophobic group, as is the case with **13n**, and **13l** retains activity.

Based on the differences in potency, the best 5-substituents are electron-donating or electron-neutral. In addition, compounds with hydrophobic 4′-substituents may interact weakly with the Tyr^{1050} (Fig. 7b). No large structural changes in the protein were observed when comparing the co-crystal structures of **12m**, **13h**, **14f** and **15e**, which all have a 4-chlorophenyl group at the 3-position of the isoquinolinones but which vary in the 5-substituent. Only 10° rotation of the Tyr^{1050} side chain was observed with the 5-methoxy derivative **15e** (Fig. 7c). This methoxy group is in close contact (ca. 3 Å) to Tyr^{1071} hydroxy and to a water molecule on the protein surface (Fig. 7b). This would indicate that the methoxy group would not be the best substitution but apparently other effects overcome these unfavorable interactions. The 5-NH_2 in **12m** does not make any H-bonds with the water molecules near the binding site.

The phenyl group of **17** is rotated as described above but changes in the protein residues can also be observed when this compound is bound. Tyr^{1071} rotates by 26° on complexation with **17** and Tyr^{1050} (including the main chain atoms) moves ~0.5 Å to accommodate the 4-methyl group of the compound (Fig. 7c).

2.6. Antiproliferative activity

In very preliminary experiments, selected examples were evaluated for their antiproliferative activity against FEK4 human fibroblasts[64] and HT29 human colon adenocarcinoma cells.[65] The effects of some 5-aminoisoquinolinones on the growth of MDA-MB-231 human breast cancer cells and on LNCaP human prostate cancer cells were also assessed. The FEK4 cell line is a model for normal non-malignant cells. HT29 cells have no *BRCA* mutation but do have a class-II mutation in *APC*. It is evident (Table 3) that there is a wide range of antiproliferative activities shown by the isoquinolinones and that this activity does not correlate with potency of inhibition of the TNKSs in cell-free assays. Nevertheless, some trends can be noted. XAV939 **1** showed no inhibition of growth of either FEK4 cells or of HT29 cells under

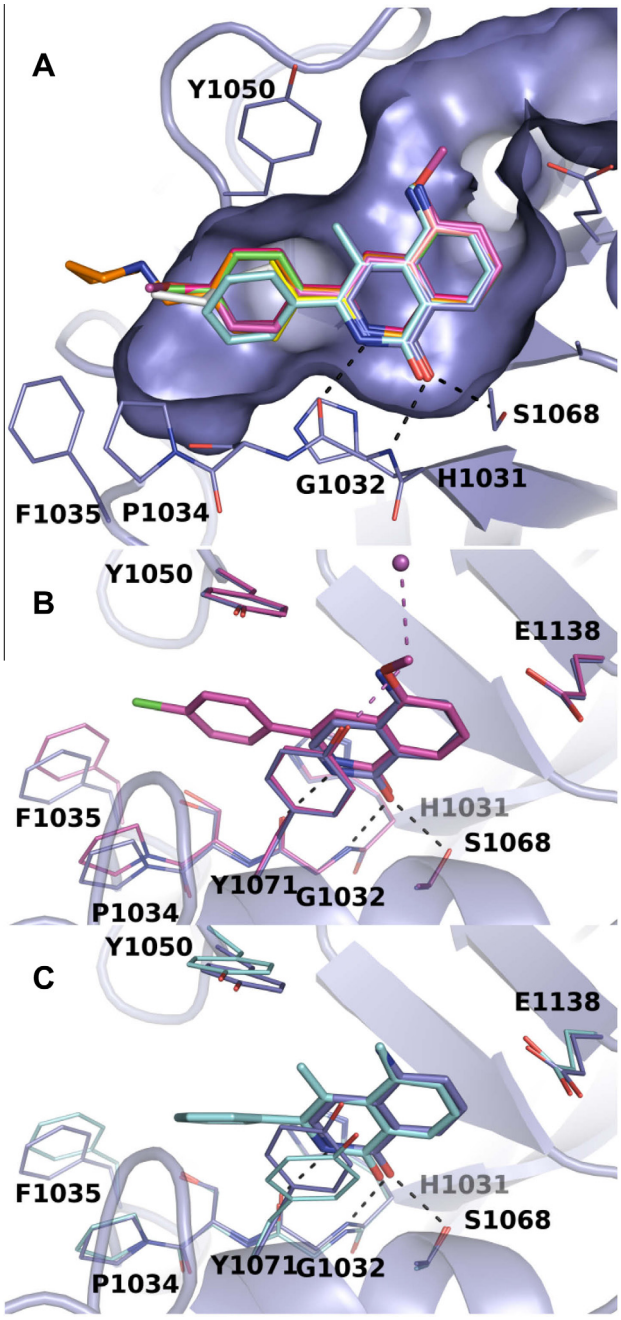

Figure 7. Co-crystal structures of tankyrase-2 with the isoquinolin-1-one inhibitors. (A) All twelve structures are superposed using the protein chain. The surface of the hydrophobic cavity, the main-chain cartoon and selected residues are shown for the complex of **11a**. Tyr^{1071} is not shown for clarity. (B) Comparison of the structures of the complexes of **11a** (blue) and **15e** (magenta). A water molecule located close to the methoxy group is shown as a sphere. (C) Comparison of the structures of the complexes of **11a** (blue) and **17** (cyan). The main-chain cartoon for the protein is shown for the structure with **11a** for panels B and C.

normal serum conditions, correlating with the findings of Huang et al.[7] for DLD-1 human colon carcinoma cells. As expected from earlier studies,[40–44,66] 5-AIQ **11a** did not inhibit the growth of any of the cell lines. The 3-ethyl analogue **11b** was similarly inactive. However, 5-aminoisoquinolin-1-ones carrying either a more substantial 3-alkyl group (**11c**) or, more effectively, a 3-aryl group (**12a**,**c**,**f**,**i**,**m**) did inhibit the growth of all the cell lines at micromolar concentrations, with no selectivity between cell types. Replacement of the 5-NH_2 group with 5-Me diminished antiproliferative activity in many cases. However, **13p**,**r**, **14** showed

Table 3
Antiproliferative activities of isoquinolin-1-ones **11**, 3-arylisoquinolin-1-ones **12**–**15**, **17** and known TNKS inhibitor **1**

Compd no.	FEK4 GI_{50} (μM)	HT29 GI_{50} (μM)	MDA-MB-231 GI_{50} (μM)	LNCaP GI_{50} (μM)
1	>500[a]	>500[a]	[b]	
11a	>200	>500	>200	>200
11b	>200	>200	101	>200
11c	49 ± 11	34 ± 7	23 ± 5	23 ± 5
11d	84 ± 7	>200	73 ± 12	51 ± 4
12a	2 ± 0.4	54 ± 7	8 ± 1	16 ± 4
12c	1.4 ± 0.4	0.65 ± 0.2		
12f	28 ± 4	85 ± 17	14 ± 4	34 ± 7
12i	59 ± 21	>100	7 ± 1	16 ± 3
12m	4 ± 1	18 ± 4	11 ± 4	10 ± 3
13b	6.0 ± 3.7	1.8 ± 0.4		
13e	>100[a]	>200[a]		
13g	>50[a]	>100[a]		
13h	48.9 ± 0.3	>200[a]		
13i	107 ± 2	38 ± 3		
13k	>50[a]	>500[a]		
13m	26.7 ± 3.3	8.2 ± 0.4		
13n	>500[a]	214 ± 16		
13p	>200[a]	12.4 ± 3.5		
13r	>500[a]	39.8 ± 8.6		
14f	>500[a]	>500[a]		
15b	>500[a]	>100[a]		
17	>200[a]	14 ± 2		

[a] Limited by solubility.
[b] Table cells without data indicate Not Determined.

selectivity for the malignant HT29 cells over "normal" FEK4 cells. Interestingly, **13b** was strongly antiproliferative against both cell types, with lesser non-selective activity shown by **13h**,**i**,**m**. Comparative studies were limited by insolubility.

Compounds **12c**, **13b**,**e**,**g**,**h**,**i**,**k**, **14b**, **13b** were selected by the National Cancer Institute for evaluation in their 60-cell line screen (Supporting information). Most showed no or very modest inhibition of proliferation of human tumour cells at 10 μM. However, the 3-(4-methylphenyl) analogues **12c** and **13b** had interesting activity against MDA-MB-435 melanoma cells and were selected for evaluation in the five-concentration screen. Compounds **13e**, **14b**, **15b** were inhibitory towards UO-31 renal cells, whereas **13g**,**h**, **14b** were active against MCF7 breast tumour cells. The five-concentration study showed that **12c** had GI_{50} = 250 nM for MDA-MB-435 cells and **13b** had GI_{50} = 316 nM for these melanoma cells and GI_{50} = 341 nM for UO-31 renal carcinoma cells.

3. Conclusions

In this paper, we report the design, synthesis and evaluation in vitro of 3-arylisoquinolin-1-ones as inhibitors of the TNKSs, using these compounds as probes of the binding site. Compounds were designed from three structural starting-points: the crystal structures of our simple PARP-1 inhibitors **11a**[40], **11b**,[51] **11c**[51] and **11d**[52] bound into the NAD^+-binding site of human TNKS-2; the crystal structure of known inhibitor **1** bound to TNKS-2;[53] 'scaffold-hopping' from our 2-arylquinazolin-4-one inhibitors of the TNKSs.[36]

3-Arylisoquinolin-1-ones were designed, carrying a variety of substituents at the 5-position. The position and nature of substituents on the 3-aryl group was also explored in this library, to help to define SAR and to explore the shape and boundaries of the hydrophobic cavity adjacent to the nicotinamide-binding Gly^{1032}/Ser^{1068} motif. To improve and generalise from our previous syntheses of 3- or 4-substituted 5-aminoisoquinolin-1-ones,[40,51,52,57,60,63] a new route was established in which the 3-aryl group was introduced from an areneboronic acid in a Suzuki–Miyaura coupling, giving diversity at a late stage. 3-Aryl-5-Me-isoquinolin-1-ones **13**, 3-aryl-5-F-isoquinolin-1-ones **14**

and 3-aryl-5-MeO-isoquinolin-1-ones **15** were assembled in one step by deprotonation of 3-substituted *N*,*N*,2-trimethylbenzamides with LDA and quench with benzonitriles; again diversity of the 3-aryl is introduced at a very late stage.

The nature of the 5-substituent in inhibition of TNKS-2 was relatively unimportant, with 5-Me and 5-OMe analogues being slightly more active than their 5-F, 5-OH or 5-NH_2 counterparts. By contrast, a (substituted)phenyl or heteroaryl group in the 3-position was essential for activity. Substitution on this 3-phenyl was also important, with groups in the *para*-position generally enhancing binding and bulky substitution in one or both *ortho*-positions abrogating activity. The electronic and polar nature of the *para*-substituent was less important; long rigid linear groups were also accepted. Also tolerated in this *para*-position were extensions carrying water-solubilising tertiary aliphatic amine salts. In general, potency against TNKS-1 paralleled potency against TNKS-2, with very few exceptions; this is unremarkable, since the NAD^+-binding catalytic domains have a high degree of sequence identity. Most of the 3-arylisoquinolin-1-ones inhibited the TNKSs highly selectively, with much lower potency against a related enzyme, PARP-1. Many of the most potent inhibitors of the TNKSs showed >500-fold selectivity for TNKS-2 versus PARP-1, with the most selective, **14b**, **15b**, being >2000-fold selective. Interestingly, the SAR for inhibition of PARP-1 and of PARP-2 by these 3-arylisoquinolin-1-ones did not parallel the SAR for inhibition of TNKSs, indicating that incorporating selectivity by design was feasible. Interestingly, the 3-(pyridin-4-yl) analogue **13p** proved to be a moderately good inhibitor of PARP-1, (IC_{50} = 111 nM) and of PARP-2 (IC_{50} = 167 nM).

The SAR was rationalised by structural studies consequent to determining the crystal structures of several analogues bound into the TNKS-2 protein. Together, the SAR and the structural studies allowed good definition of the capacity of the hydrophobic cavity to accept substituted aryl groups. The *para*-extensions projected into a narrow tunnel towards the exterior, indicating that this is a direction in which to seek further binding contacts for second-generation isoquinolin-1-one inhibitors.

Some of the compounds showed antiproliferative activity, although the link with inhibition of the tankyrases was not clear. In particular, **12c** and **13b** showed good inhibition of the growth of several tumour cell lines in the NCI 60-cell-line panel.

Thus the 3-arylisoquinolin-1-ones are shown to represent a class of highly potent and selective inhibitors of the TNKSs, with IC_{50} of some examples (**13a**–**d**) in the 1–2 nM range. Adding water-solubilising substituents is only marginally deleterious to activity. This core is therefore identified as the foundation on which to build more complex inhibitors with optimised pharmaceutical and pharmacological properties.

4. Experimental

4.1. Protein crystallography

Protein crystallography experiments were carried out using human TNKS-2. The catalytic domain was expressed, purified and crystallised as previously reported.[49] Inhibitors were soaked for 24 h to 2 months into the crystals in a well solution (0.2 M Li_2SO_4, 0.1 M Tris–HCl pH 8.5, 24–26% PEG 3350) supplemented with the test compound (100 μM or 1 mM) and NaCl (0.25 M). Before collection of data, the crystals were briefly soaked in a well solution supplemented with 20% glycerol and flash frozen in liquid N_2.

Data were collected at the Diamond Light Source on beamlines I038 and I04-1 and at ESRF on beamlines ID14-1, ID23-1 and ID23-2. Diffraction data were processed and scaled with the XDS package.[68] The structures were solved using the Difference Fourier method, with the starting phases derived from the TNKS2 structure (PDB accession code 3U9H) or with molecular replacement with MOLREP[69] using the TNKS2 structure (PDB accession code 3KR7) as a starting model. REFMAC5[70] was used for refinement and COOT[71] for manual building of the model. Statistics for collection of data and for refinement are shown in the Supporting information.

4.2. Biochemical and antiproliferative evaluation

Assays of inhibition of TNKS-1, TNKS-2 and PARP-1 were performed using methods described previously.[36] Assays of inhibition of PARP-2 were performed for **11a**, **12a**,**f**,**i**,**m** using a method described previously.[63] Assays of inhibition of PARP-2 were performed for **13b**,**k**,**p**, **14b**, **15b** with human PARP-2 using a commercial kit (AMS Biosciences PARP2 Chemiluminescent Assay Kit, Catalogue # 80552, AMS Biosciences, Abingdon, Oxfordshire OX14 4SE, UK), following the protocol provided. Antiproliferative assays were conducted as described previously.[63] IC_{50} values were estimated using Sigmaplot.

4.3. Chemical synthesis

4.3.1. General

Chemical reagents, solvents and starting materials were purchased from Sigma Aldrich, Goss Scientific, Alfa Aesar and Fisher Scientific and were used without further purification. ^1H and ^{13}C NMR spectra were recorded at 400.04 MHz or 500.13 MHz for ^1H NMR, at 100.59 MHz or 125.76 MHz for ^{13}C NMR and at 376 MHz for ^{19}F NMR, using CD_3OD, $(CD_3)_2SO$ and $CDCl_3$, containing $SiMe_4$. Reactions were monitored by thin-layer chromatography (TLC) on silica gel. MS data were obtained using electrospray ionisation on a microTOF instrument (Bruker Daltonics, Germany) and calibrated using sodium formate. Mps were measured using a hot-stage microscope (Reichert-Jung) and are uncorrected. Experiments were conducted at ambient temperature, unless otherwise noted. Solutions in organic solvents were dried with $MgSO_4$. Pd_2dba_3 refers to tris(dibenzylideneacetone)dipalladium; SPhos refers to 2-dicyclohexylphosphino-2′,6′-dimethoxybiphenyl. The brine was saturated. Compounds for biological evaluation were shown by HPLC and ^1H NMR to be >97% pure.

Compounds **11a**–**d**,[40,51,52] **12a**,**c**,**f**,**m**[51] were prepared as described previously. The syntheses of **12e**,**g**,**h**–**l**,**n**,**p**,**s**,**u**, **13c**–**k**,**m**–**r**, **14b**–**d**,**f**–**h**, **15b**–**i**, **16b**, **27**, **30b**,**d**,**e**,**h**–**n**,**q**,**r**, **31e**,**g**–**l**,**n**,**p**,**r**,**s**, **33**, **34**, **36i**,**j**, **43**, **45a**–**d**, **47**, **49**, **51** are reported in the Supporting information.

4.3.2. 5-Amino-3-(2-methoxyphenyl)isoquinolin-1-one hydrobromide (12d)

Compound **31d** (33.5 mg, 120 μmol) was stirred with HBr in AcOH (33%, 1.1 mL) at 65 °C for 5 h. Evaporation yielded **12d** (31 mg, 72%) as a pale buff solid: mp 172–175 °C; ^1H NMR (CD_3OD) δ 3.91 (3H, s, Me), 6.79 (1H, d, J = 0.5 Hz, 4-H), 7.11 (1H, td, J = 7.5, 0.9 Hz, Ph 5-H), 7.18 (1H, d, J = 8.3 Hz, Ph 3-H), 7.52 (1H, td, J = 7.6, 1.7 Hz, Ph 4-H), 7.56 (1H, dd, J = 7.6, 1.7 Hz, Ph 6-H), 7.62 (1H, t, J = 7.9 Hz, 7-H), 7.82 (1H, dd, J = 7.7, 1.2 Hz, 6-H), 8.44 (1H, d, J = 7.3 Hz, 8-H); ^{13}C NMR (CD_3OD) (HSQC/HMBC) δ 56.20 (Me), 99.86 (4-C), 112.74 (Ph 3-C), 122.06 (Ph 5-C), 124.11 (Ph 1-C), 127.25 (8a-C), 127.33 (4a-C), 127.54 (7-C), 128.60 (6-C), 129.33 (8-C), 131.26 (Ph 6-C), 132.91 (Ph 4-C), 134.01 (5-C), 142.77 (3-C), 158.49 (Ph 2-C), 163.82 (1-C); MS m/z 267.1126 $(M+H)^+$ ($C_{16}H_{15}N_2O_2$ requires 267.1135).

4.3.3. 5-Amino-3-(3-aminocarbonylphenyl)isoquinolin-1-one hydrobromide (12t)

Compound **31q** (11.2 mg, 40 μmol) was stirred with HBr in AcOH (33%, 1.5 mL) at 65 °C for 16 h. Evaporation yielded **12t**

(13.5 mg, 98%) as an amber solid: mp >360 °C; IR (KBr) ν_{max} 3351, 3173, 1664 cm^{-1}; ^1H NMR ($(CD_3)_2SO$) δ 4.2 (3H, br, $^+NH_3$), 7.11 (1H, s, 4-H), 7.43 (2H, m, Ph 4,5-H_2), 7.55 (1H, br, CON*H*H), 7.61 (1H, t, *J* = 7.7 Hz, 7-H), 7.95 (3H, m, 6,8-H_2 + Ph 6-H), 8.03 (1H, br, CONH*H*), 8.32 (1H, s, Ph 2-δ), 11.63 (1H, s, 2-H); ^{13}C NMR ($(CD_3)_2SO$) (HSQC/HMBC) δ 98.16 (4-C), 121.83 (Ph 3-C), 122.64 (Ph 5-C), 125.83 (Ph 2-C), 126.00, 126.85 (Ph 4-C), 128.26 (8-C), 128.87 (7-C), 129.29 (Ph 6-C), 133.85, 134.93, 139.18 (3-C), 162.33 (1-C), 167.52 ($CONH_2$); MS *m*/*z* 278.0947 $(M-H)^-$ ($C_{16}H_{12}N_3O_2$ requires 278.0930).

4.3.4. 5-Methyl-3-phenylisoquinolin-1-one (13a)

BuLi (1.6 M in hexanes, 0.90 mL, 1.4 mmol) was added to dry Pr^i_2NH (172 mg, 1.7 mmol) in dry THF (2.0 mL) at −78 °C and the mixture was stirred at −78 °C for 10 min. Compound **41** (250 mg, 1.4 mmol) in dry THF (2.0 mL) was added and the mixture was stirred for 1 h at −78 °C. PhCN (144 mg, 1.4 mmol) in dry THF (2.0 mL) was added at −78 °C and the mixture was stirred for 1 h at −78 °C, then at 20 °C for 2 h. Water (1.0 mL) was added. The mixture was extracted with CH_2Cl_2. The extract was washed thrice with brine and dried. Evaporation gave **13a** (68 mg, 20%) as white crystals: mp 214–215 °C; ^1H NMR ($(CD_3)_2SO$) (COSY/NOESY) δ 2.56 (3H, s, Me), 6.86 (1H, s, 4-H), 7.37 (1H, t, *J* = 7.7 Hz, 7-H), 7.49 (3H, m, Ph 3,4,5-H_3), 7.56 (1H, d, *J* = 7.1 Hz, 6-H), 7.82 (2H, dd, *J* = 6.6, 1.6 Hz, Ph 2,6-H_2), 8.07 (1H, d, *J* = 8.0 Hz, 8-H), 11.60 (1H, s, N-H); ^{13}C NMR ($(CD_3)_2SO$)) (HSQC/HMBC) δ 18.76 (Me), 100.00 (4-C), 124.57 (8-C), 125.00 (8a-C), 125.90 (7-C), 126.86 (Ph 2,6-C_2), 128.72 (Ph 3,5-C_2), 129.21 (Ph 4-C), 133.20 (6-C), 133.75 (4a-C), 134.20 (Ph 1-C), 136.61 (5-C), 139.87 (3-C), 162.94 (1-C); MS *m*/*z* 258.0834 $(M+Na)^+$ ($C_{16}H_{13}NNaO$ requires 258.0889).

4.3.5. 5-Methyl-3-(4-methylphenyl)isoquinolin-1-one (13b)

BuLi (1.6 M in hexanes, 0.9 mL, 1.4 mmol) was added to dry Pr^i_2NH (172 mg, 1.7 mmol) in dry THF (2.0 mL) at −78 °C and the mixture was stirred at −78 °C for 10 min. Compound **41** (250 mg, 1.4 mmol) in dry THF (2.0 mL) was added and the mixture was stirred for 1 h at −78 °C. 4-MePhCN (164 mg, 1.4 mmol) in dry THF (2.0 mL) was added at −78 °C and the mixture was stirred for 1 h at −78 °C, then at 20 °C for 16 h. Water (1.0 mL) was added. The mixture was diluted with CH_2Cl_2, washed (brine, 3×) and dried. Evaporation and recrystallisation (EtOH) gave **13b** (90 mg, 26%) as off-white crystals: mp 205–207 °C; ^1H NMR ($(CD_3)_2SO$) (COSY) δ 2.36 (3H, s, Ph-Me), 2.55 (3H, s, 5-Me), 6.82 (1H, s, 4-H), 7.30 (2H, d, *J* = 8.0 Hz, Ph 3,5-H_2), 7.35 (1H, t, *J* = 7.6 Hz, 7-H), 7.54 (1H, d, *J* = 7.2 Hz, 6-H), 7.72 (2H, d, *J* = 8.2 Hz, Ph 2,6-H_2), 8.06 (1H, d, *J* = 8.0 Hz, 8-H), 11.54 (1H, br, N-H); ^{13}C NMR ($(CD_3)_2SO$) (HSQC/HMBC) δ 18.86 (Ph-Me), 20.85 (5-Me), 99.48 (4-C), 124.62 (8-C), 124.89 (8a-C), 125.79 (7-C), 126.76 (Ph 2,6-C_2), 129.36 (Ph 3,5-C_2), 131.38 (Ph 1-C), 133.23 (6-C), 133.69 (4a-C), 136.77 (5-C), 138.94 (Ph 4-C), 139.92 (3-C), 163.05 (1-C); MS *m*/*z* 250.1226 $(M+H)^+$ ($C_{17}H_{16}NO$ requires 250.1232).

4.3.6. 3-(4-Dimethylaminomethylphenyl)-5-methylisoquinolin-1-one hydrochloride (13l)

BuLi (1.6 M in hexanes, 0.7 mL, 1.1 mmol) was stirred with dry Pr^i_2NH (142 mg, 1.4 mmol) in dry THF (2.0 mL) at −78 °C for 10 min. Compound **41** (200 mg, 1.1 mmol) in dry THF (2.0 mL) was added and the mixture was stirred for 1 h at −78 °C. Compound **45a** (181 mg, 1.1 mmol) in dry THF (2.0 mL) was added and the mixture was stirred for 1 h at −78 °C, then at 20 °C for 16 h. Water (1.0 mL) was added. The mixture was diluted with CH_2Cl_2. This mixture was washed (brine, 3×) and dried. The evaporation residue was washed (EtOH) to give **13l** (15 mg, 4%) as a white solid: mp 169–170 °C. The solid was then treated for 16 h with aq HCl (6.0 M, 2.0 mL). Evaporation and drying gave the HCl salt as a white solid: mp 292–293 °C; IR ν_{max} 3426, 1634 cm^{-1}; ^1H NMR ($(CD_3)_2SO$) δ 2.17 (6H, s, NMe_2), 2.56 (3H, s, 5-Me), 3.44 (2H, s, CH_2), 6.85 (1H, s, 4-H), 7.36 (1H, t, *J* = 7.7 Hz, 7-H), 7.40 (2H, d, *J* = 8.3 Hz, Ph 3,5-H_2), 7.55 (1H, d, *J* = 7.2 Hz, 6-H), 7.78 (2H, d, *J* = 8.3 Hz, Ph 2,6-H_2), 8.06 (1H, d, *J* = 8.0 Hz, 8-H), 11.50 (1H, br, NH); ^{13}C NMR ($(CD_3)_2SO$) (HSQC/HMBC/DEPT) δ 18.80 (5-Me), 45.05 (NMe_2), 62.97 (CH_2), 99.76 (4-C), 124.59 (8-C), 124.95 (8a-C), 125.84 (7-C), 126.66 (Ph 2,6-C_2), 129.00 (Ph 3,5-C_2), 132.78 (Ph 4-C), 133.21 (6-C), 133.73 (4a-C), 136.69 (5-C), 139.76 (Ph 1-C), 140.33 (3-C), 162.97 (1-C); MS *m*/*z* 595.3227 (2M+H) ($C_{38}H_{42}N_4O_2$ requires 595.3230), 293.1668 $(M+H)^+$ ($C_{19}H_{21}N_2O$ requires 293.1654).

4.3.7. 3-Ferrocenyl-5-methylisoquinolin-1-one (13s)

BuLi (2.5 M in hexanes, 0.46 mL, 1.1 mmol) was stirred with dry Pr^i_2NH (127 mg, 1.3 mmol) in dry THF (2.0 mL) at −78 °C for 10 min. Compound **41** (200 mg, 1.1 mmol) in dry THF (2.0 mL) was added and the mixture was stirred for 1 h at −78 °C. Ferrocenenitrile **47** (238.5 mg, 1.1 mmol) in dry THF (2.0 mL) was added and the mixture was stirred for 1 h at −78 °C, then at 20 °C for 16 h. Water (1.0 mL) was added. The mixture was diluted with CH_2Cl_2 and washed (brine, 3×). Drying and evaporation gave **13s** (80.5 mg, 21%) as a dark orange solid: mp >360 °C; IR ν_{max} 3454, 1633 cm^{-1}; ^1H NMR ($(CD_3)_2SO$) (COSY) δ 2.50 (3H, s, Me), 4.16 (5H, s, Fc′-H_5), 4.45 (2H, s, Fc 3,4-H_2), 5.11 (2H, s, Fc 2,5-H_2), 6.72 (1H, s, 4-H), 7.30 (1H, t, *J* = 7.3 Hz, 7-H), 7.50 (1H, d, *J* = 6.6 Hz, 6-H), 8.02 (1H, d, *J* = 7.7 Hz, 8-H), 11.08 (1H, br, NH); ^{13}C NMR ($(CD_3)_2SO$) (HSQC/HMBC) δ 18.81 (Me), 66.33 (Fc 2,5-C_2), 69.59 (Fc′-C_5), 69.74 (Fc 3,4-C_2), 78.61 (Fc 1-C), 97.03 (4-C), 124.44 (8a-C), 124.69 (8-C), 124.91 (7-C), 132.74 (4a-C), 133.12 (6-C), 136.96 (5-C), 140.01 (3-C), 162.74 (1-C); MS *m*/*z* 366.0552 $(M+Na)^+$ ($C_{20}H_{17}{}^{56}FeNNaO$ requires 366.0557).

4.3.8. 5-Fluoro-3-phenylisoquinolin-1-one (14a)

BuLi (1.6 M in hexanes, 0.9 mL, 1.4 mmol) was stirred with dry Pr^i_2NH (172 mg, 1.7 mmol) in dry THF (2.0 mL) at −78 °C for 10 min. Compound **49** (250 mg, 1.4 mmol) in dry THF (2.0 mL) was added and the mixture was stirred for 1 h at −78 °C. PhCN (142 mg, 1.4 mmol) in dry THF (2.0 mL) was added at −78 °C and the mixture was stirred for 1 h at −78 °C, then at 20 °C for 16 h. Water (1.0 mL) was added. The mixture was diluted with CH_2Cl_2, washed (brine, 3×) and dried. Evaporation and recrystallisation (EtOH) gave **14a** (113 mg, 34%) as an off-white solid: mp 216–217 °C; ^1H NMR ($(CD_3)_2SO$) (COSY) δ 6.91 (1H, s, 4-H), 7.55 (4H, m, 7-H + Ph 3,4,5-H_3), 7.66 (1H, m, 6-H), 7.87 (2H, m, Ph 2,6-H_2), 8.10 (1H, d, *J* = 7.9 Hz, 8-H), 11.84 (1H, br, NH); ^{13}C NMR ($(CD_3)_2SO$) (HSQC/HMBC) δ 94.80 (d, *J* = 5.3 Hz. 4-C), 117.64 (d, *J* = 19.3 Hz, 6-C), 122.78 (d, *J* = 3.4 Hz, 8-H), 126.61 (d, *J* = 3.3 Hz, 8a-C), 126.82 (d, *J* = 7.9 Hz, 7-C), 126.95 (d, *J* = 16.4 Hz, 4a-C), 126.96 (Ph 2,6-C_2), 128.83 (Ph 3,5-C_2), 129.64 (Ph 4-C), 133.59 (Ph 1-C), 141.40 (3-C), 157.31 (d, *J* = 247.8 Hz, 5-C), 161.78 (d, *J* = 2.8 Hz, 1-C); ^{19}F NMR ($(CD_3)_2SO$) δ -121.96 (dd, *J* = 9.9, 5.2 Hz, F); MS *m*/*z* 238.0670 $(M-H)^-$ ($C_{15}H_9FNO$ requires 238.0668).

4.3.9. 5-Methoxy-3-phenylisoquinolin-1-one (15a)

BuLi (1.6 M in hexanes, 0.8 mL, 1.3 mmol) was stirred with dry Pr^i_2NH (156 mg, 1.55 mmol) in dry THF (2.0 mL) at −78 °C for 10 min. Compound **51** (250 mg, 1.3 mmol) in dry THF (2.0 mL) was added and the mixture was stirred for 1 h at −78 °C. PhCN (133 mg, 1.3 mmol) in dry THF (2.0 mL) was added and the mixture was stirred for 1 h at −78 °C, then at 20 °C for 16 h. Water (1.0 mL) was added. The mixture was diluted with CH_2Cl_2, washed (brine, 3×) and dried. Evaporation and recrystallisation (EtOH) gave **15a** (97 mg, 30%) as pale peach-coloured crystals: mp 219–220 °C; ^1H NMR ($(CD_3)_2SO$) (COSY) δ 3.94 (3H, s, Me), 6.94 (1H, s, 4-H), 7.27 (1H, dd, *J* = 8.0, 0.8 Hz, 6-H), 7.43 (1H, t, *J* = 8.0 Hz, 7-H), 7.47 (3H, m, Ph 3,4,5-H_3), 7.77 (3H, m, 8-H + Ph 2,6-H_2), 11.59 (1H, br, N-

H); ^{13}C NMR ($(CD_3)_2SO$) (HSQC/HMBC) δ 55.94 (Me), 96.95 (4-C), 112.28 (6-C), 118.23 (8-C), 125.81 (4a-C), 126.68 (Ph 2,6-C_2), 126.85 (7-C), 128.40 (8a-C), 128.83 (Ph 3,5-C_2), 129.23 (Ph 4-C), 134.07 (Ph 1-C), 139.62 (3-C), 154.39 (5-C), 162.50 (1-C); MS *m*/*z* 274.0846 $(M+Na)^+$ ($C_{16}H_{13}NaNO_2$ requires 274.0844).

4.3.10. 5-Hydroxy-3-phenylisoquinolin-1-one (16a)

Compound **15a** (25 mg, 0.10 mmol) was heated with BBr_3 in CH_2Cl_2 (1.0 M, 2.0 mL) at reflux for 16 h. The evaporation residue was treated with aq NaOH (2.5 M, 3.5 mL) at 0 °C and the mixture was stirred at 20 °C for 3 h. The solution was acidified with aq HCl (2 M). The solid was collected by filtration. Chromatography (EtOAc/petroleum ether 2:3 → 1:1) gave **16a** (20 mg, 84%) as a pale yellow solid: mp 248–249 °C; IR ν_{max} 3410, 3318, 1677 cm^{-1}; ^{1}H NMR (CD_3OD) δ 7.11 (1H, dd, *J* = 7.8, 1.0 Hz, 6-H), 7.19 (1H, d, *J* = 0.6 Hz, 4-H), 7.33 (1H, t, *J* = 7.9 Hz, 7-H), 7.45 (1H, t, *J* = 8.5 Hz, Ph 4-H), 7.51 (2H, t, *J* = 8.6 Hz, Ph 3,5-H_2), 7.72 (2H, d, *J* = 8.4 Hz, Ph 2,6-H_2), 7.79 (1H, dt, *J* = 8.1, 0.8 Hz, 8-H); ^{13}C NMR (CD_3OD) (HSQC/HMBC) δ 100.75 (4-C), 117.44 (6-C), 118.52 (8-C), 126.97 (4a-C), 127.65 (Ph 2,6-C_2), 128.25 (7-C), 129.73 (8a-C), 130.10 (Ph 3,5-C_2), 130.30 (Ph 4-C), 136.05 (Ph 1-C), 139.93 (3-C), 154.58 (5-C), 165.74 (1-C); MS *m*/*z* 497.1477 (2M+Na) ($C_{30}H_{22}N_2NaO_4$ requires 497.1478), 260.0689 (M+Na) ($C_{15}H_{11}NNaO_2$ requires 260.0689), 238.0883 (M+H) ($C_{15}H_{12}NO_2$ requires 238.0868); MS *m*/*z* 236.0705 $(M-H)^-$ ($C_{15}H_{10}NO_2$ requires 236.0712).

4.3.11. 4,5-Dimethyl-3-phenylisoquinolin-1-one (17)

sec-BuLi (1.4 M in cyclohexane, 0.47 mL, 0.66 mmol) was added to **52** (115 mg, 0.6 mmol) in dry THF (1.0 mL) at −78 °C and the mixture was stirred at −78 °C for 30 min. PhCN (62 mg, 0.6 mmol) in dry THF (1.0 mL) was added and the mixture was stirred for 1 h at −78 °C, then at 20 °C for 16 h. The mixture was then cooled to 0 °C and quenched with D_2O (0.11 mL, 6.0 mmol) and stirred for 10 min. The mixture was diluted with CH_2Cl_2 and washed thrice with brine. Drying, evaporation and washing (EtOH) gave **17** (19.5 mg, 13%) as a white solid: mp >360 °C; IR ν_{max} 3453, 1644 cm^{-1}; ^{1}H NMR ($(CD_3)_2SO$) (COSY) δ 2.25 (3H, s, 4-Me), 2.76 (3H, s, 5-Me), 7.37 (1H, t, *J* = 6.8 Hz, 7-H), 7.47 (5H, m, Ph-H_5), 7.53 (1H, d, *J* = 7.1 Hz, 6-H), 8.18 (1H, d, *J* = 6.9 Hz, 8-H), 11.21 (1H, br, NH); ^{13}C NMR ($(CD_3)_2SO$) (HSQC/HMBC) δ 18.98 (4-Me), 24.54 (5-Me), 108.26 (4-C), 125.52 (8-C), 125.86 (7-C), 127.04 (8a-C), 128.33 (Ph 3,5-C_2), 128.65 (Ph 4-C), 129.74 (Ph 2,6-C_2), 134.92 (4a-C), 135.65 (Ph 1-C), 136.41 (6-C), 138.17 (5-C), 138.34 (3-C), 161.39 (1-C); MS *m*/*z* 250.1219 $(M+H)^+$ ($C_{17}H_{16}NO$ requires 250.1232).

4.3.12. 5-Nitro-3-phenylisoquinolin-1-one (22a)

Compound **30d** (38.5 mg, 140 μmol) was stirred with HBr in AcOH (33%, 1.0 mL) at 65 °C for 16 h. Evaporation yielded **22a** (23 mg, 63%) as yellow needles: mp >340 °C; ^{1}H NMR ($(CD_3)_2SO$) δ 7.22 (1H, s, 4-H), 7.51 (3H, m, Ph 3,4,5-H_3), 7.64 (1H, t, *J* = 8.0 Hz, 7-H), 7.76 (2H, m, Ph 2,6-H_2), 8.46 (1H, d, *J* = 8.0 Hz, 6-H), 8.57 (1H, d, *J* = 8.2 Hz, 8-H), 12.03 (1H, s, NH); ^{13}C NMR ($(CD_3)_2SO$) (HSQC/HMBC) δ 97.46 (4-C), 125.73 (7-C), 126.61 (8a-C), 127.21 (Ph 2,6-C_2), 128.95 (Ph 3,4,5-C_3), 130.19 (6-C), 131.60 (4a-C), 133.54 (8-C), 144.39 (5-C), 155.90 (1-C); MS *m*/*z* 265.0619 $(M-H)^-$ ($C_{15}H_9N_2O_3$ requires 265.0613).

4.3.13. 3-Chloro-1-methoxy-5-nitroisoquinoline (28)

Na (700 mg, 31.5 mmol) was added to **27** (6.0 g, 25 mmol) in dry MeOH (90 mL). The mixture was boiled under reflux for 16 h. The solvent was evaporated until 20 mL remained. $CHCl_3$ was added and the solution was washed (water, 3×). Drying and evaporation gave **28** (4.8 g, 82%) as fine yellow needles: mp 177–179 °C; ^{1}H NMR ($CDCl_3$) δ 4.20 (3H, s, Me), 7.62 (1H, t, *J* = 7.9 Hz, 7-H), 8.14 (1H, s, 3-H), 8.52 (1H, dd, *J* = 7.8, 1.3 Hz, 6-H), 8.59 (1H, dt, *J* = 8.3 Hz, 1.2 Hz, 8-H); ^{13}C NMR ($CDCl_3$) (HSQC/HMBC) δ 55.06 (Me), 108.70 (C-4), 119.44 (C-8a), 125.00 (C-7), 129.32 (C-6), 131.49 (C-8), 131.95 (C-4a), 147.40 (C-3), 160.86 (C-1); MS *m*/*z* 239.0216 $(M+H)^+$ ($C_{10}H_8{}^{35}ClN_2O_3$ requires 239.0223).

4.3.14. 3-Chloro-5-nitroisoquinolin-1-one (29)

Compound **28** (505 mg, 2.1 mmol) was stirred with HBr/AcOH (33%, 1.0 mL) at 65 °C for 16 h. Evaporation and recrystallisation (EtOAc) yielded **29** (211 mg, 44%) as yellow needles: mp 271–272 °C; ^{1}H NMR ($CDCl_3$) δ 7.25 (1H, s, 4-H), 7.68 (1H, t, *J* = 8.0 Hz, 7-H), 8.48 (1H, dd, *J* = 8.0, 1.5 Hz, 6-H), 8.53 (1H, ddd, *J* = 7.0, 1.5, 0.5 Hz, 8-H), 12.82 (1H, s, N-H); ^{13}C NMR ($CDCl_3$) (HSQC/HMBC) δ 102.65 (4-C), 126.29 (7-C), 130.19 (6-C), 130.76 (4a,8a-C_2), 133.63 (8-C), 143.63 (5-C), 146.61 (3-C), 160.84 (1-C); MS *m*/*z* 222.9870 $(M-H)^-$ ($C_9H_4{}^{35}ClN_2O_3$ requires 222.9910).

4.3.15. 1-Methoxy-5-nitro-3-phenylisoquinoline (30a)

Degassed PhMe (3.5 mL) was added to **28** (144 mg, 0.60 mmol), Pd_2dba_3 (57 mg, 60 μmol), SPhos (57 mg, 120 μmol), $PhB(OH)_2$ (115 mg, 0.91 mmol) and K_3PO_4 (266 mg, 1.2 mmol) in a dry flask. The mixture was stirred at 100 °C for 2 d. The evaporation residue, in $CHCl_3$, was filtered. Chromatography (EtOAc/petroleum ether 1:24), followed by chromatography (EtOAc/petroleum ether 1:29) gave **30a** (142 mg, 84%) as a bright yellow solid: mp 160–166 °C; ^{1}H NMR ($CDCl_3$) δ 4.28 (3H, s, Me), 7.49 (4H, m, Ph 3,4,5-H_3, 7-H), 8.20 (2H, dd, *J* = 8.5, 1.5 Hz, Ph 2,6-H_2), 8.47 (1H, dd, *J* = 7.8, 1.3 Hz, 6-H), 8.51 (1H, s, 4-H), 8.60 (1H, dt, *J* = 8.2, 1.1 Hz, 8-H); ^{13}C NMR ($CDCl_3$) (HSQC/HMBC) δ 54.43 (Me), 105.41 (4-C), 120.29 (8a-C), 124.72 (7-C), 127.42 (Ph 2,6-C_2), 128.85 (6-C), 129.02 (Ph 3,5-C_2), 129.65 (Ph 4-C), 131.49 (8-C), 131.84 (4a-C), 138.96 (Ph 1-C), 145.28 (5-C), 152.23 (3-C), 160.81 (1-C); MS *m*/*z* 281.0918 $(M+H)^+$ ($C_{16}H_{13}N_2O_3$ requires 281.0928).

4.3.16. 1-Methoxy-5-nitro-3-(2-trifluoromethylphenyl)isoquinoline (30g). Method A

Degassed PhMe (3.0 mL) was added to **28** (103 mg, 0.43 mmol), $Pd_2(dba)_3$ (42.2 mg, 46 mmol), SPhos (41.9 mg, 102 μmol), 2-$F_3CPhB(OH)_2$ (160.2 mg, 0.84 mmol) and K_3PO_4 (179 mg, 0.84 mmol) and the mixture was stirred at 100 °C for 16 h. The evaporation residue, in $CHCl_3$, was filtered. Chromatography (Et_2O/petroleum ether 1:199) gave **30g** (63 mg, 42%) as a yellow solid.

4.3.17. 1-Methoxy-5-nitro-3-(2-trifluoromethylphenyl)isoquinoline (30g). Method B

Dry DMF (5.0 mL) was added to **37** (175 mg, 620 μmol), Pd_2dba_3 (57 mg, 60 μmol), SPhos (58 mg, 120 μmol), 2-$F_3CPhB(OH)_2$ (176 mg, 930 μmol) and K_3PO_4 (394 mg, 1.9 mmol). The mixture was stirred at 135 °C for 16 h. The evaporation residue, in $CHCl_3$, was filtered (Celite®). Chromatography (EtOAc/petroleum ether 1:99 → 1:19) gave **30g** (90 mg, 42%) as a yellow solid: mp 95–99 °C; ^{1}H NMR ($CDCl_3$) δ 4.18 (3H, s, Me), 7.57 (1H, tt, *J* = 7.0, 1.4 Hz, Ph 5-H), 7.64 (3H, m, Ph 4,6-H_2 and 7-H), 7.83 (1H, d, *J* = 7.9 Hz, Ph 3-H), 8.18 (1H, s, 4-H), 8.51 (1H, dd, *J* = 7.8, 1.2 Hz, 6-H), 8.66 (1H, dt, *J* = 8.3, 1.0 Hz, 8-H); ^{13}C NMR ($CDCl_3$) (HSQC/HMBC) δ 54.44 (Me), 109.28 (4-C), 119.80 (8a-C), 124.15 (q, *J* = 270.4 Hz, CF_3), 125.11 (7-C), 126.89 (q, *J* = 5.0 Hz, Ph 3-C), 128.56 (Ph 5-C), 128.58 (6-C), 128.76 (q, *J* = 30.6 Hz, Ph 2-C), 130.86 (4a-C), 131.29 (8-C), 131.62 (Ph 6-C), 131.75 (Ph 4-C), 139.69 (Ph 1-C), 144.96 (5-C), 153.10 (3-C), 160.05 (1-C); ^{19}F NMR ($CDCl_3$) δ −56.75 (s, CF_3); MS *m*/*z* 349.0798 $(M+H)^+$ ($C_{17}H_{12}F_3N_2O_3$ requires 349.0802).

4.3.18. 3-(4-Hydroxyphenyl)-1-methoxy-5-nitroisoquinoline (30p). Method A

To **28** (102 mg, 360 μmol) was added Pd_2dba_3 (32 mg, 36 μmol), SPhos (33.5 mg, 70 μmol), 4-$HOPhB(OH)_2$ (74 mg, 540 μmol) and K_3PO_4 (229 mg, 1.1 mmol). Degassed PhMe (3.0 mL) was added and the mixture was stirred at 100 °C for 16 h. The evaporation

residue, in $CHCl_3$, was filtered (Celite®). Chromatography (EtOAc/petroleum ether 1:49 → 1:3) gave **30p** (10 mg, 9%) as a bright red solid: mp >230 °C; ^{1}H NMR ($(CD_3)_2SO$) δ 4.23 (3H, s, Me), 6.95 (2H, dd, J = 8.8, 2.0 Hz, Ph 3,5-H_2), 7.72 (1H, t, J = 8.0 Hz, 7-H), 8.08 (2H, dd, J = 8.8, 2.0 Hz, Ph 2,6-H_2), 8.24 (1H, s, 4-H), 8.59 (2H, m, 6,8-H_2). 9.87 (1H, br, OH); ^{13}C NMR ($(CD_3)_2SO$) (HSQC/HMBC) δ 54.05 (O-Me), 102.51 (4-C), 115.73 (Ph 3,5-C_2), 118.51 (8a-C), 125.13 (7-C), 128.30 (Ph 2,6-C_2), 128.79 (4a-C), 129.11 (6-C), 130.81 (8-C), 144.43 (5-C), 150.95 (3-C/Ph 1-C), 159.06 (Ph 4-C), 159.93 (1-C); MS m/z 297.0861 $(M+H)^+$ ($C_{16}H_{13}N_2O_4$ requires 297.0877).

4.3.19. 1-Methoxy-5-nitro-3-(4-hydroxyphenyl)isoquinoline (30p). Method B

To **28** (300 mg, 1.26 mmol) was added $Pd_2(dba)_3$ (115 mg, 130 μmol), SPhos (117 mg, 250 μmol), 4-HOPhB$(OH)_2$ (260 mg, 1.9 mmol) and K_3PO_4 (800 mg, 3.8 mmol). Dry DMF (7.0 mL) was added and the mixture was stirred at 135 °C for 16 h. The evaporation residue, in $CHCl_3$, was filtered (Celite®). Evaporation and chromatography (EtOAc/petroleum ether 1:49 → 2:3) gave **30p** (200 mg, 54%) as a bright red solid.

4.3.20. 3-(4-Hydroxyphenyl)-1-methoxy-5-nitroisoquinoline (30p). Method C

To **37** (101 mg, 0.36 mmol) in a dry flask was added $Pd_2(dba)_3$ (32.5 mg, 36 μmol), SPhos (33 mg, 70 μmol), 4-HOPhB$(OH)_2$ (73.5 mg, 0.53 mmol) and K_3PO_4 (226.1 mg, 1.07 mmol). Dry DMF (3.0 mL) was added and the mixture was stirred at 125 °C for 16 h. The evaporation residue, in $CHCl_3$, was filtered (Celite®). Chromatography (EtOAc/petroleum ether 1:39 → 3:17) gave **30p** (90 mg, 86%) as a bright red solid.

4.3.21. 5-Amino-1-methoxy-3-(2-methoxyphenyl)isoquinoline (31d)

Compound **30d** (40.3 mg, 140 μmol) was stirred vigorously with Pd/C (10%, 44 mg) in EtOH (9 mL) under H_2 for 5 h. Filtration (Celite®) and evaporation yielded **31d** (33.5 mg, 88%) as a pale yellow solid: mp 119–121 °C; ^{1}H NMR ($CDCl_3$) δ 3.93 (3H, s, PhOMe), 4.18 (3H, s, 1-OMe), 6.92 (1H, dd, J = 7.5, 0.8 Hz, 6-H), 7.04 (1H, d, J = 8.2 Hz, Ph 3-H), 7.12 (1H, td, J = 7.4, 1.0 Hz, Ph 5-H), 7.30 (1H, t, J = 7.8 Hz, 7-H), 7.35 (1H, td, J = 8.3, 1.8 Hz, Ph 4-H), 7.69 (1H, d, J = 8.2 Hz, 8-H), 7.93 (1H, s, 4-H), 8.14 (1H, dd, J = 7.7, 1.7 Hz, Ph 6-H); ^{13}C NMR ($CDCl_3$) (HSQC/HMBC) δ 53.55 (1-OMe), 55.79 (PhOMe), 109.00 (4-C), 111.67 (Ph 3-C), 113.74 (6-C), 114.28 (8-C), 119.15 (8a-C), 120.95 (Ph 5-C), 126.60 (7-C), 128.15 (4a-C), 128.91 (3-C), 129.04 (Ph 4-C), 131.05 (Ph 6-C), 141.42 (5-C), 144.22 (Ph 1-C), 157.20 (Ph 2-C), 160.29 (1-C); MS m/z 303.1119 $(M+Na)^+$ ($C_{17}H_{16}N_2NaO_2$ requires 303.1110).

4.3.22. 1,3-Dibromo-5-nitroisoquinoline (36)

Aq HNO_3 (67%, 78 mg, 0.87 mmol) in concd H_2SO_4 (93 mg, 0.95 mmol) at 0 °C was added dropwise to **35** (251 mg, 0.87 mmol) in concd H_2SO_4 (3.0 mL) at 0 °C. The mixture was stirred at 0 °C for 2H, then at 20 °C for 1H, then poured onto ice. The solid was collected by filtration, washed (H_2O) and dried to yield **36** (285 mg, 98%) as a yellow solid: mp 226–228 °C; IR ν_{max} 1516, 1334, 730 cm^{-1}; ^{1}H NMR ($(CD_3)_2SO$) δ 8.00 (1H, t, J = 7.9 Hz, 7-H), 8.54 (1H, s, 4-H), 8.64 (1H, d, J = 8.6 Hz, 6-H), 8.73 (1H, dd, J = 7.8, 0.9 Hz, 8-H); ^{13}C NMR ($(CD_3)_2SO$) (HSQC/HMBC) δ 119.57 (4-C), 126.19 (4a-C), 128.93 (7-C), 130.41 (8a-C), 130.64 (8-C), 135.28 (6-C), 135.58 (3-C), 144.09 (1-C), 144.76 (5-C).

4.3.23. 3-Bromo-1-methoxy-5-nitroisoquinoline (37)

Na (403 mg, 17.5 mmol) was dissolved in dry MeOH (10 mL); this solution was added to **36** (969 mg, 2.9 mmol) in dry MeOH (10 mL). The mixture was boiled under reflux for 24 h. EtOAc was added to the cooled mixture and the solution was washed (brine, 3×). Evaporation and recrystallisation (MeOH) gave **33** (516 mg, 74%) as a yellow solid: mp 188–192 °C; IR ν_{max} 1563, 1356 cm^{-1}; ^{1}H NMR ($CDCl_3$) (NOESY) δ 4.15 (3H, s, Me), 7.58 (1H, t, J = 8.1 Hz, 7-H), 8.26 (1H, s, 4-H), 8.46 (1H, dd, J = 7.8, 1.2 Hz, 6-H), 8.53 (1H, dd, J = 8.2, 0.9 Hz, 8-H); ^{13}C NMR ($CDCl_3$) (HSQC/HMBC) δ 55.06 (Me), 112.64 (4-C), 119.42 (4a-C), 125.11 (7-C), 129.17 (6-C), 131.49 (8-C), 131.71 (8a-C), 137.45 (3-C), 143.75 (5-C), 160.25 (1-C).

4.3.24. 1-Methoxy-5-nitro-3-(2-phenylethynyl)isoquinoline (38)

To **37** (100 mg, 350 μmol) in a dry flask was added $(Ph_3P)_2PdCl_2$ (12.6 mg, 18 μmol), CuI (6.7 mg, 35 μmol) and sodium ascorbate (4.0 mg, 20 μmol). Degassed THF (3.0 mL) and Pr^i_2NH (2.0 mL) were added and the mixture was stirred at 50 °C for 30 min, after which phenylethyne (72 mg, 0.35 mmol) was added. The mixture was stirred for 16 h at 50 °C. The solvents were evaporated. The residue, in $CHCl_3$, was filtered (Celite®). Chromatography (EtOAc/petroleum ether 1:99 → 1:19) gave **38** (100 mg, 93%) as a bright yellow solid: mp 153–154 °C; ^{1}H NMR ($CDCl_3$) δ 4.22 (3H, s, Me), 7.38 (3H, m, Ph 3,4,5-H_3), 7.60 (1H, t, J = 8.0 Hz, 7-H), 7.64 (2H, m, Ph 2,6-H_2), 8.32 (1H, s, 4-H), 8.48 (1H, dd, J = 7.8, 1.2 Hz, 6-H), 8.59 (1H, dt, J = 7.1, 1.0 Hz, 8-H); ^{13}C NMR ($CDCl_3$) (HSQC/HMBC) δ 54.63 (Me), 89.26 (ethyne 2-C), 90.14 (ethyne 1-C), 113.94 (4-C), 120.27 (4a-C), 122.19 (Ph 1-C), 125.51 (7-C), 128.39 (Ph 3,4,5-C_3), 128.82 (6-C), 130.52 (8a-C), 131.30 (8-C), 132.13 (Ph 2,6-C_2), 137.55 (3-C), 144.15 (5-C), 160.76 (1-C); MS m/z 305.0901 $(M+H)^+$ ($C_{18}H_{13}N_2O_3$ requires 305.0928).

4.3.25. 5-Amino-1-methoxy-3-(2-phenylethyl)isoquinoline (39)

Compound **38** (65 mg, 210 μmol) was stirred vigorously with Pd/C (10%, 71 mg) in EtOH (5.0 mL) under H_2 for 6 h. Filtration (Celite®) and evaporation gave **39** (51 mg, 87%) as a pale buff oil; ^{1}H NMR ($CDCl_3$) δ 3.15 (4H, m, CH_2CH_2), 4.15 (Me), 6.88 (1H, dd, J = 7.5, 1.0 Hz, 6-H), 6.90 (1H, s, 4-H), 7.26 (6H, m, 7-H + Ph-H_5), 7.69 (1H, d, J = 8.5 Hz, 8-H); ^{13}C NMR ($CDCl_3$) (HSQC/HMBC) δ 35.65 (ethyl 1-C), 39.92 (ethyl 2-C), 53.47 (Me), 105.65 (4-C), 113.64 (6-C), 114.38 (8-C), 118.79 (4a-C), 125.72 (Ph 4-C), 125.85 (7-C), 128.24 (Ph 2,6-C_2), 128.30 (8a-C), 128.51 (Ph 3,5-C_2), 140.79 (5-C), 142.17 (Ph 1-C), 150.72 (3-C), 160.69 (1-C); MS m/z 279.1560 $(M+H)^+$ ($C_{17}H_{16}N_2O$ requires 279.1499).

4.3.26. 2,3,*N*,*N*-Tetramethylbenzamide (41)

$SOCl_2$ (3.0 g, 25 mmol) was added to 2,3-dimethylbenzoic acid **40** (1.00 g, 6.7 mmol) at 0 °C. The mixture was heated at reflux for 16 h. The evaporation residue, in CH_2Cl_2 (1.0 mL), was added dropwise to Me_2NH in water (40%, 3.7 mL) at 0–20 °C. The mixture was stirred at 20 °C for 1 h, diluted with CH_2Cl_2, washed (water, 3×) and dried. Evaporation gave **41** (990 mg, 84%) as a pale yellow oil: ^{1}H NMR ($CDCl_3$) (COSY/NOESY) δ 2.16 (3H, s, 2-Me), 2.27 (3H, s, 3-Me), 2.81 (3H, s, N-Me), 3.12 (3H, s, N-Me′), 6.99 (1H, dd, J = 7.2, 1.8 Hz, 4-H), 7.10 (1H, t, J = 7.5 Hz, 5-H), 7.13 (1H, dd, J = 7.6, 1.8 Hz, 6-H); ^{13}C NMR ($CDCl_3$) (HSQC/HMBC) δ 16.00 (2-Me), 20.03 (3-Me), 34.48 (N-Me′), 38.37 (N-Me), 123.40 (4-C), 125.82 (5-C), 130.01 (6-C), 132.25 (2-C), 137.02 (1-C), 137.42 (3-C), 171.99 (C=O); MS m/z 178.1226 $(M+H)^+$ ($C_{11}H_{16}NO$ requires 178.1232).

4.3.27. 2-Ethyl-*N*,*N*,3-trimethylbenzamide (52)

BuLi (1.6 M in hexanes, 1.65 mL, 2.6 mmol) was stirred with dry Pr^i_2NH (463 mg, 3.3 mmol) in dry THF (2.0 mL) at −78 °C for 10 min. Compound **41** (390 mg, 2.2 mmol) in dry THF (3.0 mL) was added and the mixture was stirred for 1 h at −78 °C. MeI (343 mg, 2.4 mmol) in dry THF (2.0 mL) was added and the mixture was stirred for 1 h at −78 °C, then at 20 °C for 16 h. Water (1.0 mL) was added. The mixture was diluted with CH_2Cl_2. This mixture was

washed (brine, 3×) and dried. Evaporation and chromatography (EtOAc/petroleum ether 1:9 → 1:1) gave **52** (100 mg, 24%) as a colourless oil: ^{1}H NMR ($CDCl_3$) (COSY/NOESY) δ 1.14 (3H, t, J = 7.6 Hz, CH_2*Me*), 2.34 (3H, s, 3-Me), 2.60 (2H, m, CH_2), 2.81 (3H, s, NMe), 3.13 (3H, s, NMe), 6.96 (1H, d, J = 7.3 Hz, 4-H), 7.10 (1H, t, J = 7.5 Hz, 5-H), 7.14 (1H, d, J = 7.3 Hz, 6-H); ^{13}C NMR ($CDCl_3$) (HSQC/HMBC/DEPT) δ 14.25 (CH_2*Me*), 19.26 (3-Me), 23.55 (CH_2), 34.56 (NMe), 38.91 (NMe), 123.62 (4-C), 125.84 (5-C), 130.74 (6-C), 136.64 (3-C), 136.92 (1-C), 138.52 (2-C), 171.98 (C=O); MS m/z 192.1491 $(M+H)^+$ ($C_{12}H_{17}NO$ requires 192.1310).

Acknowledgements

We are very grateful to the Association for International Cancer Research (now Worldwide Cancer Research) for generous funding of this project (10-0104). Protein crystallography work was funded by Biocenter Oulu and Academy of Finland (Grant No. 251314 for L.L. and Grant No. 266922 for T.H.). We also thank Dr. Timothy J. Woodman (University of Bath) for help with the NMR spectra and Ciara O'Mahony (School of Pharmacy & Pharmaceutical Sciences, Trinity College, Dublin, Ireland) for improving the syntheses of key intermediates **30**, **31**, **34**. Protein crystallography experiments were performed on the ID14-1, ID23-1 and ID23-2 beamlines at the European Synchrotron Radiation Facility (ESRF), Grenoble, France and at the Diamond Light Source (Didcot, UK) beamlines I038 and I04-1. We are grateful to local contacts at ESRF and at Diamond for providing assistance in using beamlines. The research leading to these results has received funding from the European Community's Seventh Framework Programme (FP7/2007-2013) under BioStruct-X (Grant agreement N° 283570).

Supplementary data

Supplementary data associated with this article can be found, in the online version, at http://dx.doi.org/10.1016/j.bmc.2015.06.061.

References and notes

1. Smith, S.; Giriat, I.; Schmitt, A.; de Lange, T. *Science* **1998**, *282*, 1484.
2. Cook, B. D.; Dynek, J. N.; Chang, W.; Shostak, G.; Smith, S. *Mol. Cell. Biol.* **2002**, *22*, 332.
3. Seimiya, H.; Muramatsu, Y.; Smith, S.; Tsuruo, T. *Mol. Cell. Biol.* **2004**, *24*, 1944.
4. Javle, M.; Curtin, N. J. *Br. J. Cancer* **2011**, *105*, 1114.
5. Chang, P.; Coughlin, M.; Mitchison, T. J. *Nat. Cell Biol.* **2005**, *7*, 1133.
6. Kim, W.; Kim, M.; Jho, E.-H. *Biochem. J.* **2013**, *450*, 9.
7. Huang, S.-M. A.; Mishina, Y. M.; Liu, S.; Cheung, A.; Stegmeier, F.; Michaud, G. A.; Charlat, O.; Wiellette, E.; Zhang, Y.; Wiessner, S.; Hild, M.; Shi, X.; Wilson, C. J.; Mickanin, C.; Myer, V.; Fazal, A.; Tomlinson, R.; Serluca, F.; Shao, W.; Cheng, H.; Shultz, M.; Rau, C.; Schirle, M.; Schlegl, J.; Ghidelli, S.; Fawell, S.; Lu, C.; Curtis, D.; Kirschner, M. W.; Lengauer, C.; Finan, P. M.; Tallarico, J. A.; Bouwmeester, T.; Porter, J. A.; Bauer, A.; Cong, F. *Nature* **2009**, *461*, 614.
8. Kaminker, P. G.; Kim, S.-H.; Taylor, R. D.; Zebarjadian, Y.; Funk, W. D.; Morin, G. B.; Yaswen, P.; Campisi, J. *J. Biol. Chem.* **2001**, *276*, 35891.
9. Sbodio, J. I.; Lodish, H. F.; Chi, N.-W. *Biochem. J.* **2002**, *361*, 451.
10. Martínez, P.; Blasco, M. A. *Nat. Rev. Cancer* **2011**, *11*, 161.
11. Broccoli, D.; Smogorzewska, A.; Chong, L.; de Lange, T. *Nat. Genet.* **1997**, *17*, 231.
12. Klingelhutz, A. J. *Anticancer Res.* **1999**, *19*, 4823.
13. Sahin, E.; DePinho, R. A. *Nature* **2010**, *464*, 520.
14. Chang, S. *Aging* **2010**, *2*, 639.
15. Dynek, J. N.; Smith, S. *Science* **2004**, *304*, 97.
16. Smith, S.; de Lange, T. *J. Cell Sci.* **1999**, *112*, 3649.
17. Yeh, T.-Y. J.; Sbodio, J. I.; Chi, N.-W. *Biochem. Biophys. Res. Commun.* **2006**, *350*, 574.
18. Chang, W.; Dynek, J. N.; Smith, S. *Biochem. J.* **2005**, *391*, 177.
19. Kim, M. K.; Smith, S. *Mol. Biol. Cell* **2014**, *25*, 30.
20. Gelmini, S.; Poggesi, M.; Distante, V.; Bianchi, S.; Simi, L.; Luconi, M.; Casini Raggi, C.; Cataliotti, L.; Pazzaglia, M.; Orlando, C. *Cancer Lett.* **2004**, *216*, 81.
21. Sidorova, N.; Zavalishina, L.; Kurchashova, S.; Korsakova, N.; Nazhimov, V.; Frank, G.; Kuimov, A. *Cell Tissue Res.* **2006**, *323*, 137.
22. Gelmini, S.; Poggesi, M.; Pinzani, P.; Ciullini Mannurita, S.; Cianci, F.; Valanzano, R.; Orlando, C. *Oncol. Rep.* **2006**, *16*, 1261.
23. Shebzukhov, Y. V.; Lavrik, I. N.; Karbach, J.; Khlgatian, S. V.; Koroleva, E.; Belousov, P. V.; Kashkin, K. N.; Knuth, A.; Jager, E.; Chi, N.-W.; Kuprash, D. V.; Nedospasov, S. A. *Cancer Immunol. Immunother.* **2008**, *57*, 871.
24. Campbell, L. J.; Fidler, C.; Eagleton, H.; Peniket, A.; Kusec, R.; Gal1, S.; Littlewood, T. J.; Wainscoat, J. S.; Boultwood, J. *Leukemia* **2006**, *20*, 671.
25. Shervington, A.; Patel, R.; Lu, C.; Cruickshanks, N.; Lea, R.; Roberts, G.; Dawson, T.; Shervington, L. *Brain Res.* **2007**, *1134*, 45.
26. Tang, B.; Wang, J.; Fang, J.; Jiang, B.; Zhang, M.; Wang, Y.; Yang, Z. *J. Clin. Neurosci.* **2012**, *19*, 139.
27. Gao, J.; Zhang, J.; Long, Y.; Tian, Y.; Lu, X. *Br. J. Cancer* **2006**, *94*, 341.
28. Gelmini, S.; Quattrone, S.; Malentacchi, F.; Villari, D.; Travaglini, F.; Giannarini, G.; Della Melina, A.; Pazzagli, M.; Nicita, G.; Selli, C.; Orlando, C. *Clin. Chem. Lab. Med.* **2007**, *45*, 862.
29. Seimiya, M. *Br. J. Cancer* **2006**, *94*, 341.
30. Anastas, J. N.; Moon, R. T. *Nat. Rev. Cancer* **2013**, *13*, 11.
31. Lehtiö, L.; Chi, N.-W.; Krauss, S. *FEBS J.* **2013**, *280*, 3576.
32. Haikarainen, T.; Krauss, S.; Lehtiö, L. *Curr. Pharm. Des.* **2014**, *20*, 6472.
33. Waaler, J.; Machon, O.; Tumova, L.; Dinh, H.; Korinek, V.; Wilson, S. R.; Paulsen, J. E.; Pedersen, N. M.; Eide, T. J.; Machonova, O.; Gradl, D.; Voronkov, A.; von Kries, J. P.; Krauss, S. *Cancer Res.* **2012**, *72*, 2822.
34. Li, Z.; Yamauchi, Y.; Kamakura, M.; Murayama, T.; Goshima, F.; Kimura, H.; Nishiyama, Y. *J. Virol.* **2012**, *86*, 492.
35. Lau, T.; Chan, E.; Callow, M.; Waaler, J.; Boggs, J.; Blake, R. A.; Magnuson, S.; Sambrone, A.; Schutten, M.; Firestein, R.; Machon, O.; Korinek, V.; Choo, E.; Diaz, D.; Merchant, M.; Polakis, P.; Holsworth, D. D.; Krauss, S.; Costa, M. *Cancer Res.* **2013**, *73*, 3132.
36. Nathubhai, A.; Wood, P. J.; Lloyd, M. D.; Thompson, A. S.; Threadgill, M. D. *ACS Med. Chem. Lett.* **2013**, *4*, 1173.
37. Haikarainen, T.; Koivunen, J.; Narwal, M.; Venkannagari, H.; Obaji, E.; Joensuu, P.; Pihlajaniemi, T.; Lehtiö, L. *ChemMedChem* **2013**, *8*, 1978.
38. Narwal, M.; Haikarainen, T.; Fallarero, A.; Vuorela, P. M.; Lehtiö, L. *J. Med. Chem.* **2013**, *56*, 3507.
39. Narwal, M.; Koivunen, J.; Haikarainen, T.; Obaji, E.; Legala, O. E.; Venkannagari, H.; Joensuu, P.; Pihlajaniemi, T.; Lehtiö, L. *J. Med. Chem.* **2013**, *56*, 7880.
40. McDonald, M. C.; Mota-Filipe, H.; Wright, J. A.; Abdelrahman, M.; Threadgill, M. D.; Thompson, A. S.; Thiemermann, C. *Br. J. Pharmacol.* **2000**, *130*, 843.
41. Szabó, G.; Bährle, S.; Stumpf, N.; Sonnenberg, K.; Szabó, E.; Pacher, P.; Csont, T.; Schulz, R.; Dengler, T. J.; Liaudet, L.; Jagtap, P. G.; Southan, G. J.; Vahl, C. F.; Hagl, S.; Szabó, C. *Circ. Res.* **2002**, *90*, 100.
42. Chatterjee, P. K.; Chatterjee, B. E.; Pedersen, H.; Sivarajah, A.; McDonald, M. C.; Mota-Filipe, H.; Brown, P. A. J.; Stewart, K. N.; Cuzzocrea, S.; Threadgill, M. D.; Thiemermann, C. *Kidney Int.* **2004**, *65*, 499.
43. Genovese, T.; Mazzon, E.; Muià, C.; Patel, N. S. A.; Threadgill, M. D.; Bramanti, P.; De Sarro, A.; Thiemermann, C.; Cuzzocrea, S. *J. Pharmacol. Exp. Ther.* **2005**, *312*, 449.
44. Genovese, T.; Mazzon, E.; Di Paola, R.; Muià, C.; Threadgill, M. D.; Caputi, A. P.; Thiemermann, C.; Cuzzocrea, S. *J. Pharmacol. Exp. Ther.* **2005**, *313*, 529.
45. Bregman, H.; Gunaydin, H.; Gu, Y.; Schneider, S.; Wilson, C.; DiMauro, E. F.; Huang, X. *J. Med. Chem.* **2013**, *56*, 1341; Hua, Z.; Bregman, H.; Buchanan, J. L.; Chakka, N.; Guzman-Perez, A.; Gunaydin, H.; Huang, X.; Gu, Y.; Berry, V.; Liu, J.; Teffera, Y.; Huang, L.; Egge, B.; Emkey, R.; Mullady, E. L.; Schneider, S.; Andrews, P. S.; Acquaviva, L.; Dovey, J.; Mishra, A.; Newcomb, J.; Saffran, D.; Serafino, R.; Strathdee, C. A.; Turci, S. M.; Stanton, M.; Wilson, C.; DiMauro, E. F. *J. Med. Chem.* **2013**, *56*, 10003.
46. Narwal, M.; Venkannagari, H.; Lehtiö, L. *J. Med. Chem.* **2012**, *55*, 1360.
47. Qiu, W.; Lam, R.; Voytyuk, O.; Romanov, V.; Gordon, R.; Gebremeskel, S.; Vodsedalek, J.; Thompson, C.; Beletskaya, I.; Battaile, K. P.; Pai, E. F.; Rottapel, R.; Chirgadze, N. Y. *Acta Crystallogr.* **2014**, *D70*, 2740.
48. Shultz, M. D.; Majumdar, D.; Chin, D. N.; Fortin, P. D.; Feng, Y.; Gould, T.; Kirby, C. A.; Stams, T.; Waters, N. J.; Shao, W. *J. Med. Chem.* **2013**, *56*, 7049.
49. Shultz, M. D.; Cheung, A. K.; Kirby, C. A.; Firestone, B.; Chen, C. H.; Chen, Z.; Chin, D.; DiPietro, L.; Fazal, A.; Feng, Y.; Fortin, P. D.; Gould, T.; Lagu, B.; Lei, H.; Lenoir, F.; Majumdar, D.; Ochala, E.; Palermo, M. G.; Pham, L.; Pu, M.; Smith, T.; Stams, T.; Tomlinson, R. C.; Toure, B. B.; Visser, M.; Wang, R. M.; Waters, N. J.; Shao, W. *J. Med. Chem.* **2013**, *56*, 6495.
50. Voronkov, A.; Holsworth, D. D.; Waaler, J.; Wilson, S. R.; Ekblad, B.; Perdreau-Dahl, H.; Dinh, H.; Drewes, G.; Hopf, C.; Morth, J. P.; Krauss, S. *J. Med. Chem.* **2013**, *56*, 3012.
51. Woon, E. C. Y.; Sunderland, P. T.; Paine, H. A.; Lloyd, M. D.; Thompson, A. S.; Threadgill, M. D. *Bioorg. Med. Chem.* **2013**, *21*, 5218.
52. Dhami, A.; Mahon, M. F.; Lloyd, M. D.; Threadgill, M. D. *Tetrahedron* **2009**, *65*, 4751.
53. Karlberg, T.; Markova, N.; Johansson, I.; Hammarström, M.; Schütz, P.; Weigelt, J.; Schüler, H. *J. Med. Chem.* **2010**, *53*, 5352.
54. Jagtap, P.; Szabó, C. *Nat. Rev. Drug Disc.* **2005**, *4*, 421.
55. Ferraris, D. V. *J. Med. Chem.* **2010**, *53*, 4561.
56. Suto, M. J.; Turner, W. R.; Arundel-Suto, C. M.; Werbel, L. M.; Sebolt-Leopold, J. S. *Anti-Cancer Drug Des.* **1991**, *7*, 107.
57. Woon, E. C. Y.; Dhami, A.; Sunderland, P. T.; Chalkley, D. A.; Threadgill, M. D. *Lett. Org. Chem.* **2006**, *3*, 619.
58. Woon, E. C. Y.; Dhami, A.; Mahon, M. F.; Threadgill, M. D. *Tetrahedron* **2006**, *62*, 4829.
59. Sunderland, P. T.; Thompson, A. S.; Threadgill, M. D. *J. Org. Chem.* **2007**, *72*, 7409.
60. Sunderland, P. T.; Dhami, A.; Mahon, M. F.; Jones, L. A.; Tully, S. R.; Lloyd, M. D.; Thompson, A. S.; Javaid, H.; Martin, N. M. B.; Threadgill, M. D. *Org. Biomol. Chem.* **2011**, *9*, 881.
61. Poindexter, G. S. *J. Org. Chem.* **1982**, *47*, 3187.

62. Cho, W.-J.; Park, M.-J.; Chung, B.-H.; Lee, C.-O. *Bioorg. Med. Chem. Lett.* **1998**, *8*, 41.
63. Sunderland, P. T.; Woon, E. C.; Dhami, A.; Bergin, A. B.; Mahon, M. F.; Wood, P. J.; Jones, L. A.; Tully, S. R.; Lloyd, M. D.; Thompson, A. S.; Javaid, H.; Martin, N. M. B.; Threadgill, M. D. *J. Med. Chem.* **2011**, *54*, 2049.
64. Tyrrell, R. M.; Pidoux, M. *Cancer Res.* **1986**, *46*, 2665.
65. Fogh, J.; Fogh, J. M.; Orfeo, T. J. *Natl. Cancer. Inst.* **1977**, *59*, 221.
66. Cai, L.; Threadgill, M. D.; Wang, Y.; Li, M. *Pathol. Oncol. Res.* **2009**, *15*, 323.
67. Lehtiö, L.; Collins, R.; van den Berg, S.; Johansson, A.; Dahlgren, L. G.; Hammarström, M.; Helleday, T.; Holmberg-Schiavone, L.; Karlberg, T.; Weigelt, J. *J. Mol. Biol.* **2008**, *379*, 136.
68. Kabsch, W. *J. Appl. Crystallogr.* **1993**, *26*, 795.
69. Vagin, A.; Teplyakov, A. *J. Appl. Crystallogr.* **1997**, *30*, 1022.
70. Murshudov, G. N.; Skubák, P.; Lebedev, A.; Pannu, N. S.; Steiner, R. A.; Nicholls, R. A.; Winn, M. D.; Long, F.; Vagin, A. A. *Acta Crystallogr.* **2011**, *D67*, 3557.
71. Emsley, P.; Cowtan, K. *Acta Crystallogr.* **2004**, *D60*, 2126.